

1965

Fatigue tests of welded plate girders in shear, November 1965

B. T. Yen

J. M. Mueller

Follow this and additional works at: <http://preserve.lehigh.edu/engr-civil-environmental-fritz-lab-reports>

Recommended Citation

Yen, B. T. and Mueller, J. M., "Fatigue tests of welded plate girders in shear, November 1965" (1965). *Fritz Laboratory Reports*. Paper 1863.

<http://preserve.lehigh.edu/engr-civil-environmental-fritz-lab-reports/1863>

This Technical Report is brought to you for free and open access by the Civil and Environmental Engineering at Lehigh Preserve. It has been accepted for inclusion in Fritz Laboratory Reports by an authorized administrator of Lehigh Preserve. For more information, please contact preserve@lehigh.edu.

Progress Report on the Fatigue Strength
of Welded Plate Girders

FATIGUE TESTS OF WELDED PLATE GIRDERS IN SHEAR

B. T. Yen

John A. Mueller

Draft as submitted for review

to the

Welded Plate Girder Project Subcommittee

of the

Welding Research Council

Lehigh University
Department of Civil Engineering
Fritz Engineering Laboratory Report 303.6
November, 1964

TABLE OF CONTENTS

SYNOPSIS

- I. INTRODUCTION
- II. SPECIMENS AND TEST SETUP
 - 2.1 Design Considerations
 - 2.2 Material and Geometrical Properties
 - 2.3 Characteristic Loads
 - 2.4 Setup and Instrumentation
- III. TESTING OF THE GIRDERS
 - 3.1 General Description of Testing Procedure
 - 3.2 Testing of Girder F3
 - 3.3 Testing of Girder F4
 - 3.4 Testing of Girder F5
- IV. WEB DEFLECTIONS AND STRESSES
 - 4.1 Lateral Web Deflections
 - a. Cross-Sectional Shapes of the Web
 - b. Web Contours
 - 4.2 Stresses in the Web
 - a. Stresses Normal to the Web Boundaries
 - b. Principal Web Stresses
- V. DISCUSSION
 - 5.1 The Cracks
 - a. Crack Location and Appearance
 - b. Crack Length Versus Applied Load and Girder Stiffness
 - c. "Minor" Cracks
 - 5.2 The Stresses
 - 5.3 On Future Work

303.6

ACKNOWLEDGEMENTS

TABLES

FIGURES

REFERENCES

SYNOPSIS

Fatigue tests on three large-size girders were conducted as a part of an investigation on the fatigue strength of welded plate girders. The specimens of ASTM-A373 steel were subjected to high shear and developed a failure mode which differed from that of beams. Cracks generally occurred in the web along panel boundaries and showed a tendency of propagating diagonally into the panel. Girder deflections, as well as lateral movements of the webs, were observed to understand the behavior of girders under repeated loading. In an attempt to interpret the cause of fatigue cracks, strains at various web points were recorded. The growth of cracks and effectiveness of repairs were also studied. Further study on these items is regarded essential.

I. INTRODUCTION

As a result of an investigation on the static strength of plate girders, ^(1,2,3) specifications have recently permitted more slender webs than before for girders used in buildings. Naturally, the question arose as to the possibility of extending the results on static strength to plate girders used in bridges. Would the tension field action of the web ^(2,4,5) -- responsible for the increase in the allowable web slenderness-- cause problems more serious than those normally encountered due to girder details generating fatigue failures? Preliminary tests on two large-size, welded plate girders were conducted to determine the fatigue behavior of girders loaded with high shear ⁽⁶⁾. The failure mode which developed was different than that of ordinary beams or that of girders with thicker webs. It was not readily apparent whether the tension field action, directly or indirectly, caused or promoted the fatigue failures. In order to further study the problem and compile additional data for a more extensive analytical study ⁽⁷⁾, this series of three, slender-web plate girders loaded in high shear was designed.

In this series attention was focused on the webs, particularly along panel boundaries, since all primary cracks in the two pilot tests occurred there. Instrumentation was aimed at giving the stresses at critical points along the bounding stiffeners and flanges. Cross sections at which lateral web deflections were measured were closely spaced near the boundaries in an attempt to correlate web deflections and stresses in an analytical study. Finally, it was decided to allow all cracks to grow to a considerable length in order to observe the failure mode of the girders.

It is recognized that shear is only one of the loading conditions which is normally applied to girders. Other loadings also must be

investigated before final design recommendations can be made. Preliminary tests on girders subjected to pure bending have been conducted and will be reported separately. In this report, though, only girders under high shear will be considered.

II. SPECIMENS AND TEST SETUP

2.1 Design Considerations

Three girders, designated as F3, F4 and F5, were designed to corroborate the results obtained on the two preliminary test girders, F1 and F2⁽⁷⁾, as well as to conform to equipment limitations. Figure 1 gives the dimensions of the specimens whereas Table 1 summarizes the geometrical features of all five girders. Each of the specimens had a 3/16" web at the center which was butt-welded to thicker webs at the ends. Failure was expected to occur at the central portion of a girder (referred to as the "test section") even though the entire girder was subjected to testing. For all girders, the intermediate stiffeners were 3" x 1/4" plates welded continuously to both sides of the web and to the compression flange. Plates 5" x 1/2" in size served as loading stiffeners at the quarter points and at the ends of the girders.

Girder F3 duplicated girder F2 (Table 1) except for the cover plates at the supports and the size of the loading stiffeners. The 11" x 1" cover plates of girder F2 were added to its 12" x 1" flanges at the supports to keep its deflection well within the allowable stroke of the test equipment. However, cracks occurred at the ends of these cover plates. Since the study of such cracks was not the object of the investigation in these tests, 12" x 1 1/4" plates were used as the flanges of girder F3 at the supports and were butt-welded to the adjacent 12" x 1" flanges (Fig. 1). By reducing the total thickness of flange, the bending stresses were increased at the supports, giving a more realistic balance between shear and bending stresses there.

Identical girders F4 and F5 had the same geometry for the central part as that of girder F3. The unstiffened end sections, ten feet in length, provided an opportunity to observe the behavior of long panels. To ensure tension field action in the end panels and, at the same time, to confine primary cracks to the test sections, 5/16" thick webs were used as compared with the 3/16" webs of the centers. A 10" x 3/8" end-plate, parallel to the loading stiffener, anchored the tension field action^(2,5). In order to conform again to the stroke limitation of the loading jacks, thick flanges had to be used. These 12" x 1⁵/₈" plates ran the whole length of the end sections and were butt-welded to the 12" x 1" flanges of the central section.

Because the girders were to be tested under repeated loading and, thus, subjected to the possibility of fatigue cracks at any weak points, care was taken to design girder details. Therefore, transverse and loading stiffeners were all cut short of the tension flanges. Furthermore, all flange and web butt-welds were offset from each other and from the supporting points of the girders (Fig. 1). Finally, all these welds had 1 to 2¹/₂ tapers for smooth transitions between plates of different thicknesses. By so doing, the possibility of girder failure by such details was reduced and close attention could be given to girder webs, particularly those slender webs at the test section.

In this series of test girders the sizes of all butt welds were designed in accordance with the AWS specifications whereas almost all fillet welds were smaller than those stipulated. The smaller fillet welds were adopted on the assumption that, statically, the welds would be sufficient if the sum of the throat dimensions of the two opposite welds was equal to the thickness of the thinner plate at the joint. The sizes used are indicated

in Fig. 1. Table 2 lists the processes of depositing these welds as well as the welding sequence used by the fabricator. It may be noted that, except for the flange butt welds where the submerged arc process was employed, all other welds were deposited by the semi-automatic CO₂ process.

2.2 Material and Geometric Properties

The specimens were fabricated from steel plates which conformed to the ASTM-A373 specification. In gathering the material emphasis was on obtaining yield points not higher than 39 ksi so that the intended test loads would be within the capacity of the loading system. To ensure this, short plates were cut from the component plates before fabrication and sent for approval to the Fritz Engineering Laboratory. Here tensile coupon tests were conducted and measurements of the actual plate sizes made. The results are as listed in Table 3.

In this table the chemical analyses were supplied by the fabricator. The physical properties, however, were generally determined by the investigators. It is to be noted that the yield stresses (σ_y) are the static yield levels which were obtained at zero strain rates. In fatigue testing, the strain rates are evidently not zero. But, since the strain rates differ from point to point in a girder and since the static stress is used in estimating a girder's load carrying capacity, these static yield levels are given as standard reference values. For the one inch flanges of F3 and F4 and the one and five eighth inch flanges of F5, the static yield level was not clearly obtained and the mill test results are given and so noted.

Tests were not conducted on the base metal to determine its fatigue properties. It was anticipated that fatigue cracks would appear at heat-affected zones in the web adjacent to the fillet welds along the web.

boundaries. In regard to this weldment, certain data were available as to its fatigue properties⁽⁸⁾.

Actual dimensions of component plates, which differed slightly from the nominal sizes, were used in computing the cross-sectional constants of the girders. The nominal web depth of fifty inches was essentially maintained during fabrication. In Table 4 are listed the pertinent constants for the test section and the end sections of each girder. The aspect ratio (α) is the ratio of the panel length to its depth. All test panels were square and thus had aspect ratios of 1.0. Because the webs were thicker at the ends than in the test sections, the ratio of the web depth to its thickness, or the web slenderness ratio (β), was lower for the ends. The last three columns in the table are the web area (A_w), the moment of inertia of a section (I) and the section modulus (S), all of which are computed by conventional methods.

2.3 Characteristic Loads

From the material properties and the cross-sectional constants of the girders, characteristic loads were evaluated and are listed in Table 5 for reference. These loads include the linear buckling load of a web panel under pure shear, V_{cr} , and the estimated static ultimate load of a girder, P_u . Also listed are the minimum and maximum loads, P_{min} and P_{max} , applied during fatigue testing.

The web buckling load (V_{cr}) is the critical shear force that would have to be applied to a web panel in order to cause lateral buckling of the web. It is computed as the product of the critical shearing stress, τ_{cr} , and the area of the web, A_w ⁽⁴⁾. For the reason that web buckling in

the sense of a sudden movement seldom occurs, this load is not very significant during testing. It is, however, an important reference value since the web buckling stress is the basis for current design considerations in bridge girders.

Static ultimate loads of the girders (P_u) are evaluated according to the ultimate strength theory^(1,2,3). The failure mode for all the girders was by shear at the central panels (test sections). Tension field action was incorporated in this failure mode. For the end sections, the critical ~~panels~~^{loads} of girders F4 and F5 were also controlled by shear whereas those of girder F3 had their ultimate loads dependent on an interaction between the bending and shear modes of failure⁽³⁾. It is to be remembered that all these so-called ultimate loads are the expected strengths of the girder sections if static loads would be applied to the sections.

In the determination of fatigue loads, the customary way is to specify the maximum and minimum stresses and then convert these stresses into loads. Such a procedure was not employed in this series of tests. Instead, all test loads were determined arbitrarily with reference to the static ultimate loads. This was done for the following reasons. (1) Stresses are usually specified at the most stressed points. These would be the web points along the neutral axis of a girder or at the flange web junctions according to beam theory. Such is not the case when tension field action is being considered. (2) As of yet, there is no exact analysis for the stress distribution in a web panel which contains a tension field. (3) Under tension field action, the average shearing stress in a web and the corresponding shear force can be estimated easily. (4) By referring to the static ultimate strength in shear of each girder and expressing the applied shear forces in

percentages of these ultimate strengths, some comparison among the test girders could be made.

The last two columns in Table 5 give the chosen percentages for each girder. The respective minimum loads (P_{\min}) and maximum loads (P_{\max}) are listed in the two preceding columns. Girder F3, with a minimum load of 35 percent and a maximum load of 71 percent of the static strength, had the same percentages for the test section as did girder F2. For the twin girders F4 and F5, the maximum loads equaled 65 percent of their respective ultimate loads with the minimum loads as close to zero as permitted by the stroke limitation of the loading system. A small load was required to keep the loading jacks in constant contact with the girders.

From the last two columns of Table 5 it is seen that the applied loads were lower in percentage at the end sections than at the test sections. Nowhere were the test loads above 50 percent of the static strength of the ends, except in the case of the higher loads of girder F5 which were only introduced after three million cycles of application of the lower loads. Failure at the end sections, logically, was not expected.

2.4 Setup and Instrumentation

The girders were tested in the dynamic test bed of the Fritz Engineering Laboratory. To create high shearing forces on the girders, a setup as schematically shown in Fig. 2 was adopted. The result was a constant magnitude of shearing force over the entire girder at a given load and, correspondingly, a linearly varying bending moment from zero at the center and the ends to the maximum value at the supports. The applied loads were generated by two Amsler pulsators which were synchronized to

provide a maximum magnitude of 110 kips per jack at an allowable stroke of approximately 0.4 inches. The nominal pulsating speed was 250 cycles per minute.

For the convenience of designation and reference, a coordinate system is defined in Fig. 2. The origin coincides with the central point of a girder, the X-Y plane is the middle plane of the web, and the positive Z-direction points toward the reader. Furthermore, the side of a girder with positive Z-coordinates is referred to as the near side (N.S.); the opposite side is the far side (F.S.). Thus, theoretically, the jack loads were applied at (-240, -26, 0) and (240, 26, 0) for girder F3. The three panels with X-coordinates -75 to -25, -25 to 25, and 25 to 75 are called panels 1, 2, and 3, respectively.

Lateral support for the test girders consisted of 2½ in. standard pipes at all the intermediate stiffeners of the test section at the compression side of the girders, and on the loading stiffeners adjacent to the jacks. In addition, F3 had two more pipes on the loading stiffeners at the compression flange. All pipes were pin-connected on the far side of a girder and were attached at the other end to some stationary structural members. Figure 3, a photograph of girder F4, shows the overall setup of the girders with the lateral supports behind the girder.

To detect the magnitude of stresses in a girder web under load, electrical resistance type strain gages were mounted on both sides of the web in pairs. Figure 4(a) gives the layout of the SR4-A1 gages on girders F3 and F4. The single gages were 1½ in. from the surfaces of the boundary elements, whereas those 120 degree strain rosettes were one inch from the points of convergence. In Fig. 4(b) are shown the locations of the SR4-AR1 rosettes used for girder F5. All these rosettes were ¾ in. away from the surface of the boundary elements.

Lateral deflections of web plates were measured with a dial rig that had ten Ames deflection dials with one one-thousandth of an inch divisions. The rig was calibrated against a rigid, machined, plane surface before testing and at various intervals during the tests. An accuracy of better than four-thousandths of an inch was normally obtained. Figure 4(c) gives the typical locations of the points where measurements were made in a test panel. The distances are fixed between gage points in a vertical cross section. In addition to these measurements, the movements of stiffeners along a line at $Z = 2\frac{19}{32}$ were recorded and the web deflection readings at ^{the} quarter points of all the end panels were taken.

Overall girder behavior was monitored by a one one-thousandth of an inch Ames deflection dial located under the compression flange at $X = 240$. This dial indicated the sum of the girder deflection and the vertical movement due to support settlements under load. By mounting a one-hundredth scale on each of the four bearing stiffeners at mid-height of the girder and noting their movement by an engineer's level, the support settlement could be evaluated and the girder deflection could be calculated. Since the support settlements remained constant at a given load, any change on the deflection dial reading was an indication of the overall behavior of the girder.

Because the detection of cracks was an important item, and due to the fact that the detection depended on visual observations, whitewash became necessary. Any hair line on a whitewashed surface was carefully examined to see if it was a hair crack. Local stress concentrations usually showed up as yield lines.

III. TESTING OF THE GIRDERS

3.1 General Description of Testing Procedure

With a test girder centered at the testing position, a load was applied to the girder. It was increased slowly from zero to the maximum load and then removed. In the process, the load might be released at any time for fine alignment of the jacks and the girder to avoid twisting of the specimen. Besides being used for alignment purposes, this pre-loading diminished the effects of residual stresses on subsequent strain gage readings and allowed elastic strains alone to be recorded. It also served the purpose of "settling" the supports.

After the pre-loading, a complete set of strain gage and web deflection readings was taken at zero load as reference data for later readings at various load increments. Figure 5, a load-deflection curve of girder F4, indicates the general procedure of a static test. Load numbers were assigned to each load magnitude for easy reference. Upon completing the recordings at the maximum load, a thorough inspection of the entire girder was performed. All minor yield lines at high residual stress regions were noted and a careful examination of all the welds was made to see that no crack was present.

Pulsating of the jacks began after the jack loads were reduced from the maximum value to the mean load. Approximately five minutes were required to obtain roughly the desired load magnitude and range, and a few more minutes were needed to stabilize the loads at the exact, predetermined values. At this point the counting of load cycles began and the fatigue testing was underway.

During testing, at selected time intervals of either one, two, or three hours, visual inspection of the girder was made while pulsating at 250 cycles per minute. All welded areas were examined for cracks with a three-power magnifying glass and a floodlight. Any suspected cracks would receive careful study and attention.

When the first crack was observed, the locations of its end points were marked on the girder and the corresponding coordinates were measured to the nearest sixteenth of an inch. The growth of this crack, as well as any other cracks forming later, was recorded at subsequent inspections. Testing would be stopped when a crack grew to a significant length. The jack loads were then removed and a repair effected.

After a repair, a second fatigue test was performed following the same procedure of the first test, starting with a static test and ending with the removal of the load after growth of a crack. When all three test panels had developed cracks, the test was continued until either the load dropped and the end deflection increased significantly or until the girder had withstood a total of two million load cycles after the last crack had formed. The testing of the girder was then terminated.

In general, cyclic loading was carried out on a twenty-four hour a day basis and was removed only when a repair was to be effected or when the test had been terminated. At no time was any girder left unattended for more than three hours, or about 50,000 cycles. This maximum value was relatively small when compared with the hundreds of thousands of load cycles which girders sustained before the observation of cracks.

In the next three sections the specific testing histories of girders F3, F4, and F5 will be reviewed.

3.2 Testing of Girder F3

Girder F3 was similar in geometry to girder F2 of the pilot investigation and had the same percentages of ultimate load. The static test was performed with data recorded for loads of 0, 5, 10, 20, 30, 40, 42.5 (P_{\min}), 50, 60, 70, 80 and 85 (P_{\max}) kips. By using beam theory, the maximum load produced maximum shearing stresses of 10.1 ksi in the web of the test section at $Y = 0$ and maximum bending stresses of 9.3 ksi on the flanges at $X = \pm 75$, $Y = \pm 26$. It was noted that the web at $X = 240$ was out of plumb from top to bottom by about $1\frac{1}{8}$ inches, thus inclined at an angle of $2\frac{1}{2}$ degrees off the vertical.

The pulsating load range of from 42.5 to 85 kips was next applied at an actual rate of 262.5 cycles per minute. Inspection of the girder was made at two hour intervals (every 31,500 cycles) while pulsating. After 800,000 cycles, the first crack, Crack 1, was observed with initial coordinates of $(-24\frac{3}{4}, -3\frac{7}{8}$ to $-7\frac{3}{4}, -\frac{3}{32}$). It was located in the web at the toe of the fillet weld at the intermediate stiffener. Pulsating was continued and the crack gradually propagated through the thickness of the web as well as growing vertically. At 1,150,000 cycles, when the crack was approximately fourteen inches long on both sides of the web, testing was stopped. The lower portion of the crack had begun to turn away from the stiffener and to "branch" into the web. It was decided that repair should be made at this point, even though the applied loads were being maintained and the end deflection of the girder remained practically constant.

The final appearance of Crack 1 is sketched in Fig. 6(a). Also shown are the subsequent repair ^{and} cracks. The X-coordinates of the girder are given for reference. Figure 6(b), a diagram of applied loads P versus total number of cycles of application N , may be helpful for reviewing the testing chronology.

Repair of Crack 1 began with gouging out the cracked material with a compressed air chisel and then filling in the excavation with weld beads. It was first done on one side and then on the opposite side of the web. A 5" x 3/8" plate was welded onto the far side of the web at $X = -17\frac{1}{2}$ and completed the repair. As all other intermediate stiffeners, this reinforcing stiffener was cut short of the tension flange and was welded to the compression flange. After the repair, a static test was run up to 85 kips and the fatigue test continued at the same speed and the same range as before, as indicated in Fig. 6(b).

Crack 2 was detected at 2,510,000 cycles with initial coordinates of $(74\frac{3}{4}, 2\frac{3}{8}$ to $5, \frac{3}{32})$. Like the first crack, it was on one side of the web only, developed along the toe of a stiffener fillet weld, and was in the web. Because it had no effect on the loads or the deflection of the girder, the test was continued without repair. At 2,640,000 cycles, Crack 3 was noted along the top flange of panel 1 at $(-37\frac{5}{8}$ to $-41\frac{1}{8}, 24\frac{7}{8}, -\frac{3}{32})$, horizontally. Again, the crack was located in the web along a fillet weld, on the far side. Without repairing either Crack 2 or 3, the pulsating continued up until 4,640,000 cycles. That is, the test was stopped at two million cycles after the observation of Crack 3. The final lengths of Cracks 2 and 3 are shown in Fig. 6(a). At this stage these cracks had penetrated through the web and measured about 8 inches to 13 inches, respectively, on both sides of the web. Regardless of such lengths, the loads on the girder were not affected and the girder deflection remained stable.

It is to be noted from Fig. 6(a) that all cracks had a tendency to propagate into the web, somewhat diagonally. From Fig. 6(b) it is seen that the test load was reduced to zero only once in order to repair the girder.

3.3 Testing of Girder F4

The first of the three girders tested was F4. It had a load range of practically zero to a maximum load and, thus, was used to ascertain the adequacy of the test setup. During the static test, instrument readings were taken at 0, 2, 10, 20, 30, 40, 50, 60, 70, and 82 (P_{\max}) kips. In subsequent fatigue tests, due to an appreciable deflection of the reaction frame at $X = -120$, the load range could only be set from 8 to 82 kips. Under the maximum load of 82 kips, the maximum shearing stress in the web was 8.9 ksi at $Y = 0$ and the maximum bending stresses in the test section was 9.0 ksi at $X = \pm 75$, $Y = \pm 26$.

Inspections of girder F4 were made at one hour intervals throughout the test. After 430,000 cycles of repeated load applications, Crack 1 was detected in the web of panel 3 at the toe of the stiffener fillet weld. The coordinates of the tips of the crack were $(74\frac{3}{4}, 11\frac{1}{2}$ to $15\frac{1}{4}, 3/32)$, on the near side only. At 700,000 cycles, when it became apparent that there was a tendency for the load to drop and the girder deflection to increase, the loading was stopped. The length of Crack 1 was about 12 inches on both sides of the web, as measured after stopping. Also, it was discovered that there existed another crack, Crack 2, at $(24\frac{3}{4}, 6$ to $10, 3/32)$, in the web of panel 2 along the toe of the stiffener fillet weld and only on one side of the web. Repair of Crack 1 was made by welding a 3" x 5/16" plate on each side of the web at $X = 65$ without welding the crack itself. No repair was made of Crack 2 at this time (Fig. 7).

When the pulsating load was again applied, it soon was noticed that Crack 1 continued to propagate. Since the load and the deflection were stable, testing was continued without repair. At 1,130,000 cycles, Crack 3 was observed along the top flange of panel 1, at $(-59\frac{1}{4}$ to $-62\frac{1}{4}, 24\frac{7}{8}, 3/32)$.

It was at the toe of the fillet weld, in the web. In the meantime, Crack 1 had grown across the stiffener towards the end section. To avoid damage to the web butt weld nearby, two minor reinforcing plates were put on at 1,520,000 cycles and 1,560,000 cycles (Repairs a and b) without welding Crack 1 itself. At 1,600,000 cycles, when the length of Crack 1 grew to 23 inches, a major repair (Repair c) was made by removing all previous repair plates from the web, gouging and welding the crack, and placing 24" x 21" x 3/16" web doubler plates over the crack.

With Crack 1 finally isolated, the test was continued. Crack 2 had been increasing in length ever since 700,000 cycles and, at 1,840,000 cycles, a repair of it was made when its overall length was about 13 inches. This repair (Repair 2) was done by grinding out the crack and welding it, first on one side then on the other side of the web. A pair of stiffeners, 3" x 5/16" plates, was added and welded to the web and the compression flange at $X = 17\frac{1}{2}$, as shown in Fig. 7(a).

As pulsating continued, Crack 4 occurred at $(-74\frac{3}{4}, -3$ to $-4\frac{5}{8}, -3/32)$, along the stiffener in panel 1 at 2,340,000 cycles. It again was situated in the web at the toe of the fillet weld. At 2,460,000 cycles, Crack 5 was noticed in the 3/16" web at the toe of the fillet weld of the reinforcing doubler plate, near the isolated Crack 1. This crack grew horizontally along the flange and vertically along the side of the doubler plate. The girder deflection showed a tendency to increase at 2,600,000 cycles and at about 2,900,000 cycles the load began to decrease slightly. The test was terminated at 3,100,000 cycles when the maximum load dropped to 80 kips and the end deflection had increased by about 0.06 inches (about one-quarter of the total elastic end deflection). At this time Cracks 3, 4, and 5 had final lengths of about 29, 30, and 30 inches, respectively.

Figures 7(a) and 7(b) summarize the testing and repair of girder F4. Final lengths of the cracks, except that of Crack 5, are sketched in Fig. 7(a) together with the repairs made. In Fig. 8(a), the final appearance of Crack 3 is again sketched. The growth of this crack can be traced by using Fig. 8(b), a diagram of total crack length (l) versus the number of cycles of load application after the first observations of the crack (n). (N denotes total cycles of load application on a girder). It is seen from Fig. 8(a) and (b) that, when first observed on the near side of the web, the crack had a length of about 3 inches along a flange. It propagated through the web to the far side at $n = 330,000$ cycles. Then, changing direction, it turned into the web at about 45 degrees from the horizontal. Further growing and changing direction to about 30 and 20 degrees occurred at $n = 1,470,000$ cycles and 1,800,000 cycles, respectively. As the test drew to a close, the rate of increase of crack length accelerated sharply. At the completion of the test, the crack length on both sides of the web was approximately 29 inches.

3.4 Testing of Girder F5

Girder F5 was identical to girder F4 in design and in applied loading as referred to the ultimate load. After loading to the maximum load to alleviate the effects of residual stresses and to ensure the alignment, a static test was run which included loads of 0, 4 (P_{\min}), 18, 36, 54, and 72 (P_{\max}) kips. At the maximum load, the girder was subjected to maximum shearing stresses of 8.8 ksi at $Y = 0$ and maximum bending stresses of 8.0 ksi at $X = \pm 75$, $Y = \pm 26$. The pulsating load range of from 4 to 72 kips was again applied at a rate of 262.5 cycles per minute. Inspection was made at three hour intervals.

This testing condition was continued for 192 hours, or 3,000,000 cycles, then the test was stopped for a thorough inspection for hair cracks. When no cracks were discovered, it was decided to increase the maximum load magnitude to the capacity of the loading system to force a failure. This was 110 kips and approximately equal to the predicted static strength of the girder. Thus, a second static test was made with loads of 4, 90, and 110 kips. An inspection at 110 kips still failed to reveal any cracks. A new cyclic load range of from 36 to 110 kips was then applied. Inspections were now made at two hour intervals. At 3,400,000 cycles (N), Cracks 1 and 2 were observed simultaneously, with initial coordinates of $(-24\frac{3}{4}, -2\frac{1}{8}$ to $-5\frac{3}{8}, 3/32)$ and $(34\frac{1}{2}$ to $39\frac{1}{2}, -24\frac{7}{8}, -3/32)$, respectively. Crack 1 was located in the web of panel 2 at the toe of a stiffener fillet weld; Crack 2 was along the bottom (compression) flange fillet weld of panel 3, in the web. (See Fig. 9.) These cracks grew to about 6 and 13 inches long when the test was stopped at 3,500,000 cycles for their repair. Repairs 1 and 2 consisted of gouging out and welding the cracks and placing one-sided stiffeners of 5" x 5/16" plates at X = -15 and X = 45, as indicated in Figs. 9(a) and (b).

When the repairs were completed, the cyclic loading of 36 to 110 kips was resumed. Crack 3 was first detected at 3,650,000 cycles with initial coordinates of $(-74\frac{3}{4}, -8$ to $-9\frac{3}{4}, -3/32)$. Crack 4 was noted at 3,810,000 cycles at $(-25\frac{1}{2}, -1\frac{5}{8}$ to $-3\frac{1}{2}, 3/32)$ and Crack 5 appeared at 3,870,000 cycles with coordinates of $(-25\frac{1}{2}, 12$ to $14\frac{3}{4}, -3/32)$. All three cracks were in the web of panel 1 at the toes of the fillet welds along the transverse stiffeners. Without repairing any of these cracks, pulsating was continued. At about 3,900,000 cycles the girder deflection began to increase slowly. At 4,110,000 cycles the test was terminated when the load began decreasing

and the deflection rapidly increasing. At the test's completion, Cracks 3, 4, and 5 had final lengths of about 20, 5, and 18 inches, respectively.

The crack data for all three girders is summarized in Table 6.

IV. WEB DEFLECTIONS AND STRESSES

As was discussed in the previous chapter, static tests were conducted on the specimens before fatigue loading began. During these tests, measurements of the lateral web deflections and associated web stresses were made with the instrumentation described in Section 2.4. The results obtained are described below.

4.1 Lateral Web Deflections

The lateral web deflections are presented in two ways: as cross-sectional shapes (Figs. 11, 12 and 13) and as contours (Figs. 14, 15 and 16) for girders F3, F4 and F5, respectively. The web deflections of girder F3 will be described as a typical example in the following discussion.

a. Cross-Sectional Shapes of the Web

The outline of the test section of girder F3, which includes panels 1, 2 and 3, is shown in the upper portion of Fig. 11. The X-coordinates, below the bottom flange, and the Y-coordinates, along the left-hand stiffener, are marked for reference. At a marked X-coordinate or "station", $X = -45$ for example, the thin vertical line represents a plane web's cross section. Deflected positions of a web point are plotted in respect to this line. Distances to the right of this line indicate points deflected to the near side of the girder; points to the left fall on the far side. Thus, by connecting with straight lines the appropriate points measured at a station for a particular load, a roughly drawn shape of that cross section results.

Such cross-sectional shapes are drawn for loads of 5, 42.5, and 85 kips (load numbers 2, 7, and 12, respectively). The horizontal distance between two positions of a web point indicates the movement of that web point which occurred between the two corresponding loads. Therefore, at the point $X = -45$, $Y = 9$, the lateral web deflections (w) were of the order of -0.01, 0.09, and 0.22 inches for the three loads and was about 0.13 inches between the maximum and the minimum loads of 85 and 42.5 kips. For this, as for most sections, the maximum deformed shapes conformed to the initially distorted shapes.

The three plots in the lower portion of Fig. 11 give the complete history of movement of certain points in each panel. Each point was close to the location of a crack in its respective panel. For example, the curve in the center is for the point $X = -21$, $Y = -9$, a point close to the location of the center of Crack 1 when it was first observed. Here this point on the web was initially distorted about 0.03 inches toward the near side of the girder. As load was increased, it continued to move in the positive Z-direction reaching a final value of about 0.10 inches. The partial movement from the minimum load of 42.5 kips to its maximum at 85 kips is indicated on the plot as 0.057 inches.

Deflected cross-sectional shapes such as those shown in Fig. 11, 12, and 13 depict the relative positions of cross sections at different load magnitudes. For an overview of the deflected shape of a panel, web deflection contours are presented next.

b. Web Contours

The contours of lateral web deflections of girder F3 are shown in Fig. 14 for panel 2 at three different loads: 5, 42.5, and 85 kips. A

constant contour interval of 0.03 inches is adopted. Solid lines indicate deflections to the near side of the web, dotted lines to the far side. The contours of 5 kips substantially reflected the initial web distortions present in the girder under no load. The lower portion of this panel was initially distorted toward the far side or in the negative Z-direction while the top portion was convex outward on the near side. Maximum deflections were about 0.09 and 0.12 inches on the near side and the far side, respectively. As the load was increased to 42.5 kips, the upper portion became more positive and the lower portion more negative. At the maximum load of 85 kips, the contours oriented themselves at a slope of about 25 degrees from the horizontal, and attained maximum deflection values of 0.33 and -0.27 inches. From the close spacing of the contours, it is obvious that the steepest gradients existed in the central part of the panel where cracks never occurred. The fact that a relatively steep slope was present near Crack 1, as compared with the other panel boundaries, may also be observed. The final appearance of Crack 1 is included as a reference.

Similar contours of girders F4 and F5 are given in Figs. 15 and 16. In these figures the typical contour orientation at maximum load is seen, as also is the influence of the initial deflection in predetermining the side to which the webs finally moves. In Fig. 16, the final contours of girder F5 are given for a maximum load of 72 kips. No crack is indicated in the panel, since one did not occur at this loading range which was applied for three million cycles. Only after the second load range of from 36 to 110 kips was applied, did the web crack as shown in the upper portion of Fig. 13.

4.2 Stresses in the Web

In general, the stresses considered can be divided into two categories: those caused by overall girder bending and shear and those due to out-of-plane web deflections. The first will be referred to as the primary bending membrane stresses and can be computed by the ordinary flexural formulas. On the other hand, the lateral web deflections cause both axial (membrane) and secondary plate bending stresses in the web. When stresses are obtained in experimental work through strain gages mounted on web surfaces, they are the so-called surface stresses and are the combination of membrane and plate bending stresses. By setting strain gages back to back on both sides of a web, membrane and plate bending stresses can be evaluated.

Even though the static ultimate loads of these girders were controlled by shear forces, attention is, as usual, directed toward the applied tensile stresses rather than the web shearing stresses. In the following, emphasis will be placed on the tensile stresses in the webs.

4.2.a Stresses Normal to the Web Boundaries

Because all of the cracks occurred along web boundaries and propagated there, it is natural first to examine the web stresses normal to that direction. These stresses for girder F3 are plotted in Fig. 17. They are derived from the strains at the load of 85 kips, using the small strain under the load of 5 kips as the reference. All plotted values here were obtained from strain gages whose center points were $1\frac{1}{2}$ inches away from their adjacent boundary elements. Stress was

simply computed as the product of strain and the modulus of elasticity of 29,600 ksi, neglecting Poisson's effect. The stress scale used in the figure is kept the same for all subsequent stress plots for ease of comparison.

In the upper portion of the figure, Fig. 17(a), the maximum tensile surface stresses are plotted. These stresses were found on the far side of the web at certain gage points, where an "F" is placed nearby, or otherwise they were on the near side of the girder. Small vertical index marks near the gage points at $Y = \pm 15$ indicate the magnitudes of the predicted longitudinal stresses—the primary bending stresses by beam theory. Thus, in the third panel at $X = 25\frac{5}{8}$, $Y = -15$, a surface stress of about 15 ksi is on the near side whereas its corresponding theoretical stress is about 2 ksi in compression. Further discussion of these and other stresses is presented in Section 5.2.

The central plot of Fig. 17 shows the web membrane stresses at their respective locations. Stresses less than 1 ksi are indicated by a small solid dot and negative signs adjacent to them indicate compressive stresses. It may be observed that these membrane stresses at the girder's neutral axis are as high as 7 ksi and are of the same order of magnitude on both sides of the transverse stiffeners.

Finally, in the lower part of Fig. 17, the tensile secondary bending stresses are shown. No indices of theoretical stresses are indicated, since the web is assumed planar in the beam theory. The letter "F" again indicates those stress vectors on the far side of the web. Except in a few cases, these secondary bending stresses are much larger

than their corresponding membrane stresses and, therefore, substantially represent the actual surface stresses measured at their respective locations. The largest secondary bending stress is in panel 1 at $X = -36$, $Y = 23\frac{1}{2}$ where the stress magnitude was about 23 ksi.

Presented in Fig. 18 are the web stresses of girder F4 arranged as in the previous figure. The stresses are shown for the maximum load of 82 kips, using as reference for computation the strains obtained at 2 kips. Again, all gages were $1\frac{1}{2}$ inches from the bounding elements. From the membrane stresses in the center of the figure, it is seen that the maximum tensile value is about 7 ksi and that the stresses on both sides of the stiffener at $X = -25$, $Y = 0$ are tensile and are less than 1 ksi. In Fig. 19, the web stresses of girder F5 are shown for the maximum load of 72 kips with its reference of 4 kips. All stresses were obtained by strain rosettes which were located $\frac{3}{4}$ inches from the web boundary elements. Membrane stresses were less than 3 ksi throughout and the maximum secondary bending stress was about 16 ksi near the top flange. Finally, in Fig. 20 are given the web stresses of girder F5 under its latter maximum load of 110 kips. It is interesting to note that the membrane stresses were no larger than 5 ksi, even at the maximum load of 110 kips which was the computed static strength of the girder.

After the discussion on the stresses of each girder at maximum load, the growth of the stresses with the increase of the applied loads can be illustrated by selected points in the webs of the girders. This is shown in Fig. 21 for three strain gage pairs, each pair of which was

located close to the first crack in its respective girder. The ordinate in the figure is the applied load P , in kips, and the abscissa is the measured stress, in ksi. The stress scales for girders F3 and F4 are the same whereas the scale for girder F5 is ~~half~~^{twice} that of F3 and F4. The measured surface stresses on both sides of the web are represented by the open circles. Membrane stresses, calculated from the measured surface stresses, are denoted by solid circles. The critical web buckling loads are shown for reference as obtained from Table 5. The theoretical primary bending stresses are zero for the points of upper and the lower plots, and are shown by a thin straight line in the central diagram. From these plots, it is seen that, if a load range is given, the corresponding stress range is determined. However, any given ratio of maximum load to minimum load does not equal the ratio of the corresponding maximum and minimum stresses. In the lower figure it is seen that, at 110 kips, the near side of the web had tensile surface and membrane stresses of about 2 and 22 ksi, respectively, as may also be seen in Fig. 19.

4.2.b Principal Web Stresses

Because it is possible that the principal stresses are instrumental in causing cracks, some attention will be directed toward them. By using elastic stress-strain relationships, the principal stresses at the maximum loads were computed for girders F4 and F5. The values on the surface are found in Fig. 22 and the membrane principal stresses are shown in Fig. 23. In Fig. 22, the solid vectors indicate the obtained ^{surface} stresses. The tensile stresses are plotted away from the points of measurement and the compressive stresses toward them. Beam theory

predictions are depicted by the dashed vectors. Again, the letter "F" is used to indicate stress vectors on the far side. Thus, in the third panel of girder F4, the two principal stresses are both tensile on the ^{far} ~~near~~ side of the web with the maximum value twice the magnitude of the computed beam theory value. In the two diagrams for girder F5, it is seen that the principal surface stresses generally were much greater than the beam theory values. Along the top flange, the minimum principal stresses were often tensile as opposed to the theoretical compressive values. In panel 2 of Fig. 22(c), one such tensile stress was computed to be above the material's uni-axial ^{static} ~~tensile~~ yield stress.

Corresponding to the surface stresses discussed in Fig. 22, the computed principal membrane stresses are plotted in Fig. 23. In general, there is a marked resemblance between the test values and those predicted by the beam theory. This is true in both magnitude and direction. For example, in Fig. 23(a), the tensile and compressive magnitudes are 12 ksi and 9 ksi for those computed from test data and are 11 ksi and 7 ksi according to beam theory predictions. Angular differences in Fig. 23(a) and (b) were so small as not to allow their plotting and, thus, index marks are used instead of dashed vectors to indicate stress magnitudes. Even in Fig. 23(c), for which the applied load was at the static ultimate load of the girder, stress directions did not differ by more than ten degrees and magnitudes were quite comparable to those predicted values.

5. DISCUSSION

In this section, some observations concerning the cracks and the measured stresses will be presented, followed by a short discussion in regard to future work.

5.1 The Cracks

For this discussion cracks will be referred to as either "major" or "minor". A major crack is one whose length would continually increase with the number of applied loading cycles and which would eventually cause failure of the girder. Minor cracks are those whose lengths either stop increasing at some number of cycles or whose growth rates would not be appreciable. In any case, these minor cracks do not affect either a girder's stiffness or its ability to maintain the applied loading. In sections 5.1.a and b, major cracks will be discussed whereas the locations of some minor cracks are briefly presented in section 5.1.c.

5.1.a Crack Location and Appearance

All major cracks initiated in the web of the test section along panel boundaries. Specifically, each crack when first observed was located in the web at the toe of a fillet weld (the heat-affected zone) joining the web and its bounding flanges or intermediate stiffeners. Typical initiation points are sketched in Figs. 24a and 24b for cracks along the stiffeners and flanges, respectively. As is also shown here, every major crack initiated on the surface of the web which was subjected to the tensile stresses generated by lateral web deflections.

Then, as is indicated, they progressed across the web thickness to the toe of the fillet weld on the opposite side of the web.

Figure 24c illustrates that most cracks first appeared as continuous lines parallel to a boundary. In Fig. 24d it is seen that Crack 2 of girder F4 consisted of several, small, disconnected cracks, each of whose lengths was partially parallel to the stiffener and partially inclined at some angle from the stiffener. These cracks consolidated as fatigue testing continued, propagating vertically. Later, when the crack branched into the web, it followed the path of an original small branch. This behavior of Crack 2 of girder F4 is typical of the cracks observed in the earlier tests on girders F1 and F2⁽⁶⁾. The final appearance of the cracks are sketched in Fig. 25 together with the idealized tension fields. From these sketches it may be observed that the branches of the cracks propagated into the web in a direction roughly perpendicular to the assumed tension fields.

5.1.b Crack Length Vs. Applied Load and Girder Stiffness

In general, the ability of a girder to maintain its applied load was not impaired due to its cracks when they were relatively short. However, when the final stage of growth was reached and crack lengths were about 15 to 25 inches, the pulsating load would drop. During testing, girder F3 never experienced a drop of load due to its cracks. Girder F4 had no load reduction due to Cracks 1 and 2. Only when Cracks 3, 4, and 5 had lengths of about 24, 24, and 10 inches - all existing simultaneously - did the load suddenly drop. Subjected to a maximum

load equal to its estimated ultimate load, girder F5 was unaffected by Cracks 1 and 2 while they grew to their final length. When Cracks 3, 4, and 5 had attained lengths of about 17, 5, and 16 inches, respectively, F5 could no longer maintain its load.

Changes in the overall girder stiffness are reflected in changes in the girder end deflection. As crack lengths increase to significantly large values, there is an accompanying loss of overall stiffness and the end deflection (V_e) would increase by a certain amount (ΔV_e). This increase is depicted in the uppermost portion of Fig. 26, where the changes in the end deflection (ΔV_e) are plotted against the number of applied load cycles (N). Individual ordinates are shown for each girder while the common abscissa (N) is located at the bottom of the figure. It may be noted that the effect of temperature changes or load fluctuations was the order of 0.002 inches and changes of this order are neglected. Referring to the figure, it is seen that girder F3 had no essential change in its stiffness, even though crack lengths totaled about 21 inches at the completion of the test. Girder F4 had an increase in its end deflection of about 0.006 inches at 700,000 cycles when Crack 1 was 14 inches long. After the first repair of this crack, the end deflection remained constant until 2,600,000 cycles when Cracks 3, 4, and 5 were approximately 18, 10, and 4 inches long, respectively. The final change of deflection was about 0.062 inches or 25% of the girder's maximum elastic end deflection of 0.282 inches when the crack lengths progressed to their final values of 29, 30, and 30 inches. Finally, girder F5 retained the same end deflection during the first 3,000,000

cycles when the load range was 4^k to 72^k . At 3,800,000 cycles, under the new load range of 36^k to 110^k , the end deflection began to increase. At four million cycles, when cracks 3, 4, and 5 were about 8, 4, and 9 inches long, respectively, the end deflection took a sharp turn upward and increased by a total of 0.045 inches or 13% of the elastic end deflection of 0.351 inches.

From the above results it is seen that neither the ability of a girder to maintain its applied loads nor the girder stiffness were affected by small cracks. It is interesting to speculate whether the static load carrying capacity is similarly unaffected by such small cracks.

5.1.c "Minor" Cracks

Several cracks were observed in girders F4 and F5 in addition to the major cracks described above. These cracks primarily occurred at the bearing stiffeners and reaction stiffeners adjacent to the loading jacks or reaction plates, in areas of high direct compression. The final, typical shapes of several of these cracks are shown in ~~Figure 27~~ Fig. 27 for girder F4. Detail A reveals that two cracks occurred in the web. One was located at the toe of the web-to-flange weld while the other initiated at the end of the bearing stiffener where it was clipped to provide clearance for the web-to-flange weld. The cross-sectional view of Detail A also shows that the weld joining the bearing stiffener to the compression flange was cracked through its throat and, in fact, this connection was completely severed before the end of the test. Detail B gives the final shape of a crack observed at the end

of an intermediate stiffener. This was the only one of its kind in the three girders tested. Finally, a typical crack at the loading stiffener is shown in Section C-C. The crack began in the throat of the weld on one side of the stiffener and propagated completely around the stiffener on the near side. It may be observed that these cracks were not repaired at any time during testing and had no effect on a girder's overall performance.

5.2 The Stresses

As in all human experience, an effect has been observed - the cracks. This inevitably leads to the search for the cause. Some consistent parameter should eventually be uncovered which relates crack occurrence with the number of load applications. At first, the applied load range may appear to be some measure of the number of cycles until cracks initiate. But a comparison between girders F2 and F3, both loaded within a range of $0.35 P_u$ to $0.71 P_u$, shows that cracks appeared as early as 800,000 cycles in F3 but no sooner than 2,000,000 cycles in F2. In the same light, girders F4 and F5 were both loaded from approximately $0.05 P_u$ to $0.65 P_u$. Once again, the first crack of F4 appeared at about 430,000 cycles while F5 never incurred a crack in over 3,000,000 cycles. Thus, there is little consistency in a given load range. A second parameter to be reviewed is the lateral web deflections, both initial and final. A direct comparison from panel to panel is possible because all corresponding bounding elements of the panels were nominally the same. From an examination of the web deflection contours, Figs. 14, 15, and 16, it appears that all maximum initial deflections were of the

same order of magnitude varying between + 0.06 to + 0.09 and - 0.12 to - 0.15 inches. The final contours show maximum values of + 0.33 and - 0.27, + 0.27 and - 0.24, and + 0.15 and - 0.24 inches for girders F3, F4, and F5, respectively. As with the loading, little consistency is noted between these values and the occurrence of cracks. With all other geometric and material properties essentially the same, the primary cause of cracks - stress - is the only parameter left to consider if random geometrical and metallurgical effects are excluded.

The surface stresses perpendicular to the boundaries shed very little light as to a consistent relationship between crack occurrence and number of load applications. Consider Fig. 17a, girder F3. In the upper right corner of panel 1, a tensile surface stress of about 26 ksi existed at $P = 85$ kips, with about 9 ksi at $P = 42.5$ kips, giving a stress range of about 17 ksi. This was considerably higher than the stresses in the center panel near the first crack where values of 14.5 and 3.5 ksi were obtained at the maximum and minimum loads with an accompanying range of 11 ksi. As a further example, in Fig. 20a, the maximum stress in the center panel was 31 ksi at the load range of 36^k to 110^k , while the minimum stress was about 5 ksi. This produced no cracks at that location during the application of over one million cycles of load. Thus, comparisons based on the surface stresses appear to be less than fruitful.

Do these measured stresses, which were $1\frac{1}{2}$ inches and $\frac{3}{4}$ of an inch from the boundary elements, substantially reflect the stresses which existed at the toe of the fillet weld in the web? To answer this question,

it is convenient to separate the surface stresses into their membrane components and their secondary bending components. In Fig. 17b, the membrane stresses along the neutral axis on either side of the center panel's intermediate stiffeners are essentially the same. These are 6.7 versus 6.7 ksi and 5.5 versus 4.3 ksi on either ^{side} ~~wide~~ of the stiffeners at $X = -25$ and $X = +25$, respectively. Membrane stresses along the neutral axis of +0.8 versus +1.0 ksi were also recorded for girder F4 on either side of the stiffener at $X = -25$ as is shown in Fig. 18b. These observations give some indication that the membrane stresses are essentially constant over a distance of a few inches and, thus, the membrane stresses at the gages represent the membrane stresses at the toe of the weld. With the secondary bending stresses, the opposite is true. This is because the curvature of the web at the flanges and stiffeners has little affect on the membrane stresses, whereas its affect is pronounced on the secondary web bending stresses. Further explanation is given below.

Let a small cantilever strip, one inch wide and ten inches long, be cut out of the web of girder F3 at $Y = 0$ and $X = -25$ to -15 as shown in the top sketch of Fig. 28. In this sketch the location of a pair of electrical resistance strain gages is indicated, together with the points along the neutral axis of the girder at which lateral web deflection readings were taken. The center sketch shows a plan view of the deflected web at 85 kips in relation to the web at 5 kips which is shown as being straight. For this maximum load of $P = 85$ kips, w equals 0.129, 0.195, and 0.257 inches, respectively at $X = 4, 7,$ and 10 inches. A change in the end slope of the cantilever of about 0.0185

radians occurred. Using a fourth order parabolic curve of

$$w = ax^4 + bx^3 + cx^2 + dx$$

to approximate the deflected shape of the cantilever, the secondary bending stresses are obtained and are plotted in the lower portion of Fig. 28. The bending stress at the toe of the weld is 36.1 ksi and a stress of 10.7 ksi exists at the center of the gages. From Fig. 17c, it is seen that a value of 8.0 ksi was calculated from this gage point using the measured surface stresses. Even though 36.1 ksi might be somewhat higher than the actual value of the stress at the toe of the weld, this calculation demonstrates that measured web bending stresses are much lower than those at the toe of the weld. In the case treated above the weld stress was about four times the bending stress measured at the gage.

A similar computation was made for the same girder, F3, for the gage at $X = -36$, $Y = 23\frac{1}{2}$. Due to the rigidity of the flange, it was assumed that the cantilever was fixed-ended. Using lateral web deflections at $X = -35$ and $Y = 15, 18, \text{ and } 21$ for the load of 85 kips, the secondary bending stresses are 20.1 ksi at the gage, compared with a test value of 23.2 ksi. The approximated bending stress is 30.6 ksi at the toe of the one-eighth inch fillet weld. Thus, a bending stress nearly one and one-half times the measured value at the gage exists at the weld. Again, the secondary bending stress at the gage is not indicative of the stress at the toe of the weld.

From the above, it is realized that the measured surface stresses do not adequately reflect the actual stresses existing at the toe of the weld where all major cracks occurred. Thus, further speculation as to the effects of the stresses as measured at the gage points would be fruitless. Much more extensive computation and experimentation are necessary before an intelligent discussion of the roles of the surface, membrane, and secondary bending stresses can be presented.

5.3 On Future Work

These experiments have yielded much information - both sought and unsought - and also generated many questions to be answered in later studies. The following are some considerations for future work:

1. In all tests, the web panels in the end sections never incurred a single major crack. These end panel webs were three-eighths of an inch for girder F3 and five-sixteenths of an inch for girder F4 and F5, respectively. In girder F4, these end panels were subjected to a load range of 5 to 49 percent of their ultimate load for over three million cycles. The end panels of F5 were loaded from 0.02 to 0.43 P_u for three million cycles and then from 0.21 to 0.65 P_u for an additional million cycles without developing major cracks. It is conceivable that an effect is present here which causes lower secondary bending stresses and increases fatigue life. This effect should be examined in the future.

2. Since the strain gages indicated that some combination of membrane and secondary bending stresses existed everywhere, the fatigue strength of a weldment subjected to various combinations of these stresses

should be studied. It would appear that small, welded, tee specimens would produce results useful in subsequent investigations of fatigue strength.

3. Because stresses are essential to fatigue studies, it is important to be able to calculate the stresses resulting from an applied girder loading. Tension field action, coupled with initial out-of-straightness of the web, will provide ample opportunity for analysis for some time to come. It is expected that analytical study of this problem will continue.

ACKNOWLEDGEMENTS

This investigation is a part of the welded plate girder research which has been jointly sponsored by the American Iron and Steel Institute, the American Institute of Steel Construction, the Pennsylvania Department of Highways, the U. S. Department of Commerce - Bureau of Public Roads, and the Welding Research Council. It is supervised by the Welded Plate Girder Project Subcommittee of the Welding Research Council. The financial support of the sponsors and the continued interest and guidance which the members of the subcommittee have given to the project are gratefully acknowledged.

The research work has been conducted at the Fritz Engineering Laboratory of the Civil Engineering Department, Lehigh University, Bethlehem, Pennsylvania. Professor W. J. Eney is the head and Dr. L. S. Beedle is the director of the Laboratory. Their encouragement is sincerely appreciated.

The project staff, at the time of the testing, also included Messrs. P. B. Cooper and H. S. Lew. The authors are grateful for their help and criticism. Special thanks are due to Mr. H. A. Izquierdo for preparing the figures and Miss Grace Mann and Miss Valerie Austin for typing the manuscript.

Table 1 Geometry of Test Specimens*

Girder		F1	F2	F3	F4	F5
Center	Flanges	12x1	12x1	12x1	12x1	12x1
	Web	50x3/16	50x3/16	50x3/16	50x3/16	50x3/16
	Stiffener Spacing	75	50	50	50	50
Ends	Flanges	12x1	12x1	12x1	12x1 $\frac{5}{8}$	12x1 $\frac{5}{8}$
	Web	50x3/8	50x3/8	50x3/8	50x5/16	50x5/16
	Stiffener Spacing	40	40	40	120	120
Remarks		11x1 cover plates at supports	11x1 cover plates at supports	12x1 $\frac{1}{4}$ flanges at supports	10x3/8 end plates	10x3/8 end plates

* Dimensions in inches

Table 2 Welding Details

A. Sequence

Step	Connection	Position	Weld
1	$\frac{1}{4}$ " ($\frac{5}{8}$ ") flange plates to 1" flange plates	--	a
2	3/8" (5/16") web plates to flanges	N.S.	b
	3/16" web plates to flanges	N.S.	c
3	Bearing stiff. to 3/8" (5/16") web plates	N.S.	b
	Inter. stiff. to 3/8" web plates (F3 only)	N.S.	e
	Inter. stiff. to 3/8" ^{3/16"} web plates	N.S.	c
4	3/8" (5/16") web plates to 3/16" web plates	N.S.	d
5	Same as step 2 above	F.S.	As above
6	Same as step 3 above	F.S.	As above
7	Same as step 4 above	F.S.	f

B. Welds

Weld	Type	Details	Remarks
a	Butt	S.A.; 350A, 30v, 14ipm,	5/32" dia. wire, 840 flux
b	1/4 fillet	CO ₂ , 200A, 22v, 10ipm,	
c	1/8 fillet	CO ₂ , 200A, 22v, 20ipm	
d	Butt	CO ₂ , 200A, 22v, 20ipm	0.045" dia. wire, 50 cu. ft. per in. gas flow
e	3/16 fillet	----	
f	Butt	CO ₂ , 350A, 27v, 18ipm	

Table 3 Properties of Girder Components

Girder Component			Dimensions (in.)	Chemical Analysis					Physical Properties		
				C (%)	Mn (%)	P (%)	S (%)	Si (%)	σ_y (ksi)	σ_u (ksi)	Elong. (%)
F3	Center	Flanges	12.13x1.011	0.22	0.57	0.009	0.018	0.05	36.6*	58.1	30.3
		Web	50x0.174	0.16	0.54	0.008	0.023	----	35.8	58.4	29:8
	Ends	Flanges	12.13x1.011	0.22	0.57	0.009	0.018	0.05	36.6*	58.1	30.3
		Sup. Fl. Web	12.16x1.271 50x0.378	0.15 0.17	0.55 0.56	0.010 0.008	0.022 0.023	0.23 0.03	30.8 32.4	59.8 55.9	32:2 33.5
F4	Center	Flanges	12.07x1.008	0.15	0.54	0.008	0.022	0.23	37.9*	62.0	31.3
		Web	50x0.192	0.16	0.51	0.008	0.021	0.05	33.5	56.6	31.6
	Ends	Flanges	12.29x1.636	0.16	0.77	0.009	0.021	0.20	31.6	59.9	34.0
		Web	50x0.312	--	--	---	---	--	34.4	58.8	29.7
F5	Center	Flanges	12.06x1.010	0.15	0.54	0.008	0.022	0.23	28.5	61.5	32.6
		Web	50x0.170	0.15	0.48	0.008	0.022	--	33.8	56.5	31.7
	Ends	Flanges	12.18x1.646	0.17	0.65	0.014	0.020	0.18	35.0*	62.9	32.6
		Web	50x0.312	--	--	---	---	--	34.4	58.8	29.7

* Yield points by mill tests; otherwise static yield stress levels

Table 4 Geometrical Constants

Girder		α	β	A_{web} (in. ²)	I (in. ⁴)	S (in. ³)
Center	F3	1.0	287	8.70	17770	683
	F4	1.0	260	9.60	17830	686
	F5	1.0	294	8.50	17620	677
Ends	F3	0.8	132	18.90	19890 24260*	765 923*
	F4	2.4	160	15.60	30060	1129
	F5	2.4	160	15.60	29990	1125

* At the reactions of F3

Table 5 Characteristic Loads

Girder		V_{cr} (k)	P_u (k)	P_{min} (k)	P_{max} (k)	% P_u	
						P_{min}	P_{max}
Test Section	F3	26.2	120	42.5	85	35	71
	F4	35.4	127	8	82	6	65
	F5	24.6	111	4 36*	72 110*	4 32*	65 99*
End Sections	F3	298	240	42.5	85	18	35
	F4	98	169	8	82	5	49
	F5	98	169	4 36*	72 110*	2 21*	43 65*

* Test loads changed after 3,000,000 cycles

Table 6 Summary of Crack Data

Girder	Crack	First Observance					N cycles	n cycles	Final ℓ (in.)
		Coordinates			Z	cycles			
		X	Y	Z					
F3	1	$-24\frac{7}{8}$	$-3\frac{1}{8}$ $-7\frac{3}{4}$	$-3/32$	800,000	350,000*	14*		
	2	$+74\frac{3}{4}$	$+2\frac{3}{8}$ $+5$	$+3/32$	2,510,000	2,130,000	8		
	3	$-37\frac{5}{8}$ $-41\frac{1}{8}$	$+24\frac{7}{8}$	$-3/32$	2,640,000	2,000,000	13.5		
F4	1	$+74\frac{3}{4}$	$+11\frac{1}{2}$ $+15\frac{1}{4}$	$+3/32$	430,000	1,160,000#	23#		
	2	$+24\frac{3}{4}$	$+6$ $+10$	$+3/32$	700,000	1,130,000*	13*		
	3	$-59\frac{1}{4}$ $-62\frac{1}{2}$	$+24\frac{7}{8}$	$+3/32$	1,130,000	1,980,000	29		
	4	$-74\frac{7}{8}$	-3 $-4\frac{5}{8}$	$-3/32$	2,320,000	780,000	30		
	5	---	---	$\pm 3/32$	2,460,000	640,000	29		
F5 [⊕]	1	$-24\frac{3}{4}$	$-2\frac{1}{8}$ $-5\frac{3}{8}$	$+3/32$	3,400,000	100,000*	6*		
	2	$-34\frac{1}{4}$ $+39\frac{1}{4}$	$-24\frac{7}{8}$	$-3/32$	3,400,000	100,000*	13*		
	3	$-74\frac{3}{4}$	-8 $-9\frac{3}{4}$	$-3/32$	3,650,000	460,000	20		
	4	$-25\frac{1}{4}$	$-1\frac{5}{8}$ $-3\frac{1}{2}$	$+3/32$	3,810,000	300,000	5		
	5	$-25\frac{1}{4}$	$+12$ $+14\frac{3}{4}$	$-3/32$	3,870,000	240,000	18		

* At repair

First ^{repair} crack @ n = 270,000 cycles, $\ell = 12''$

⊕ All cracks occurred in high load range (36 to 110 kips)

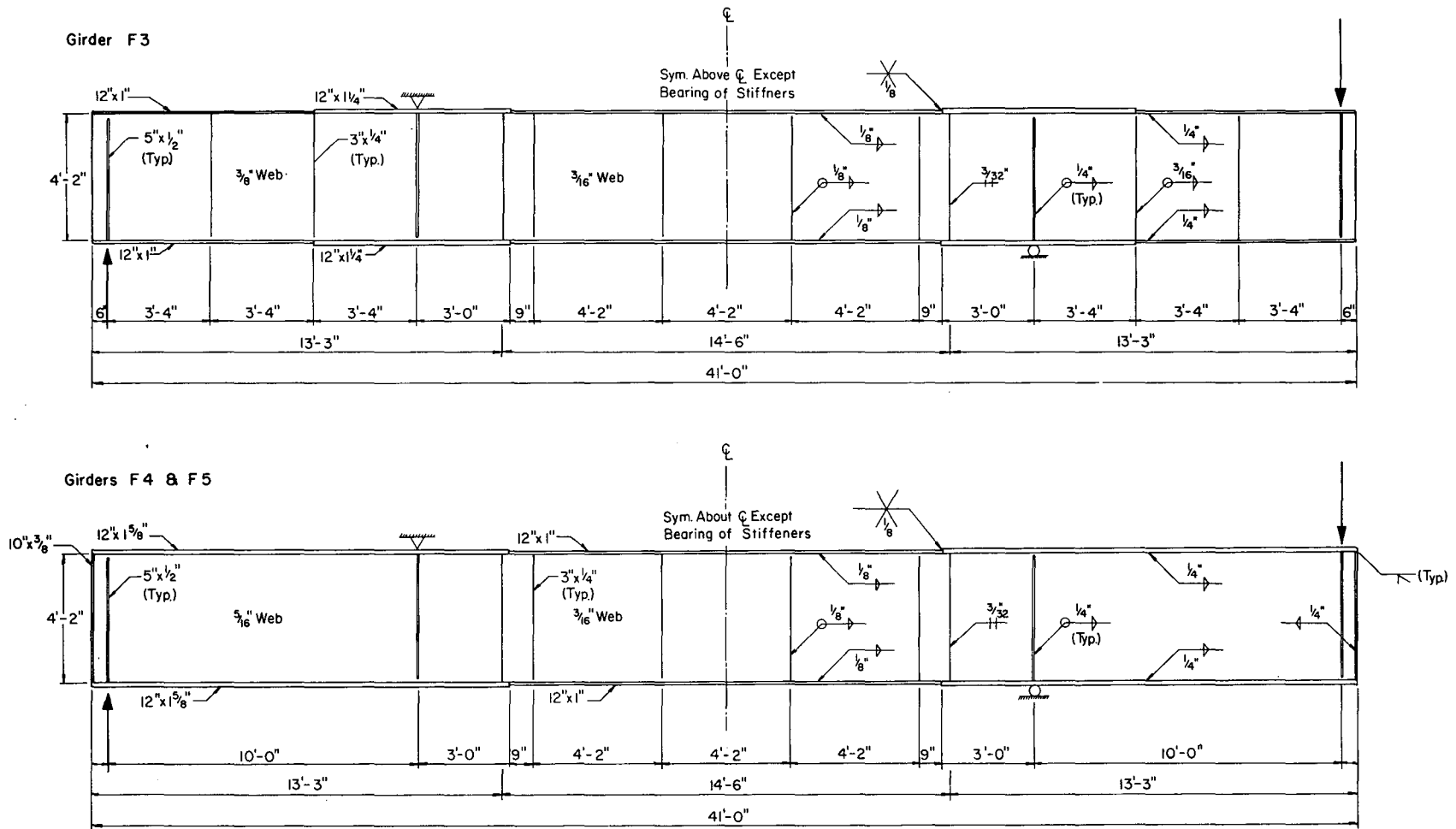


Fig. 1 Test Girders

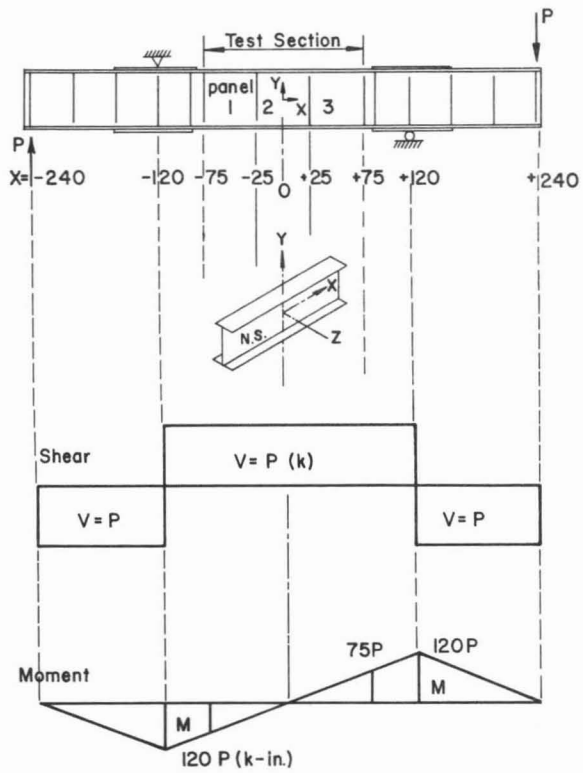


Fig. 2 Bending and Shear Diagrams

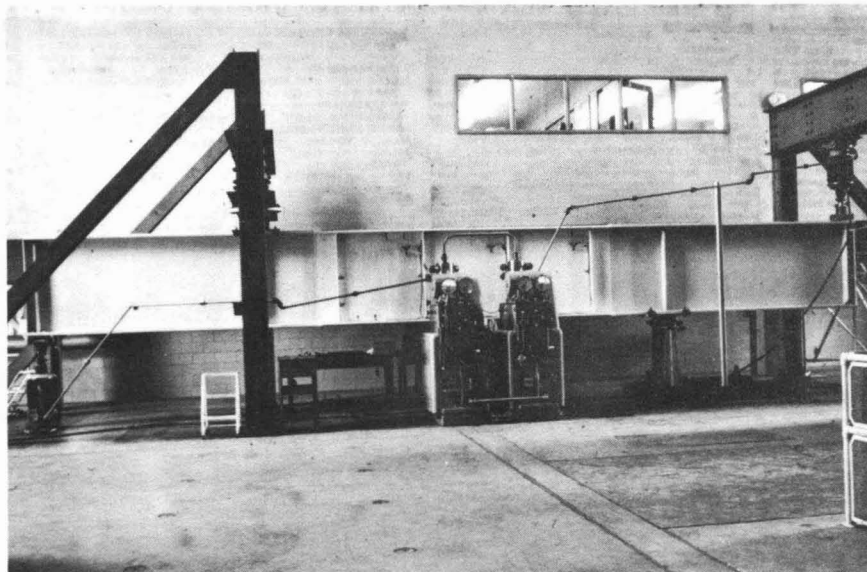
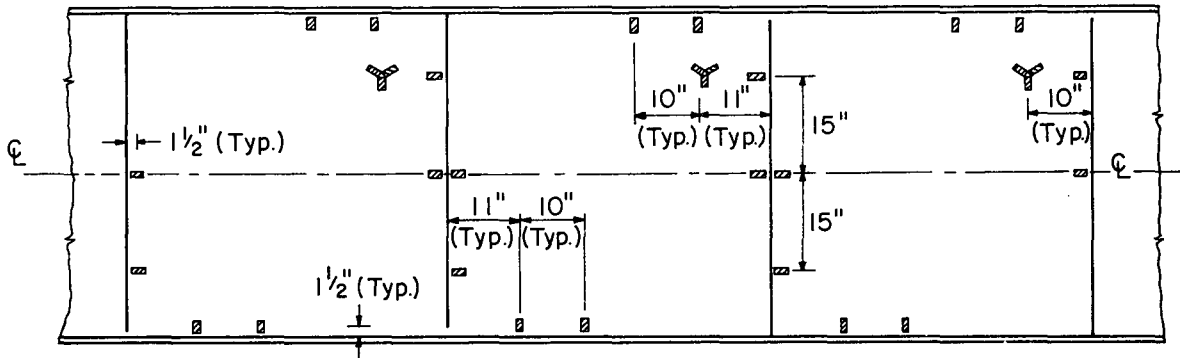
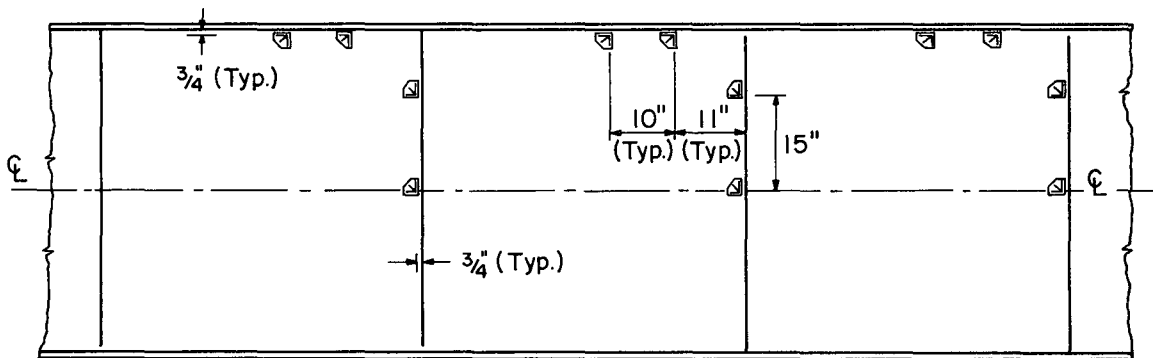


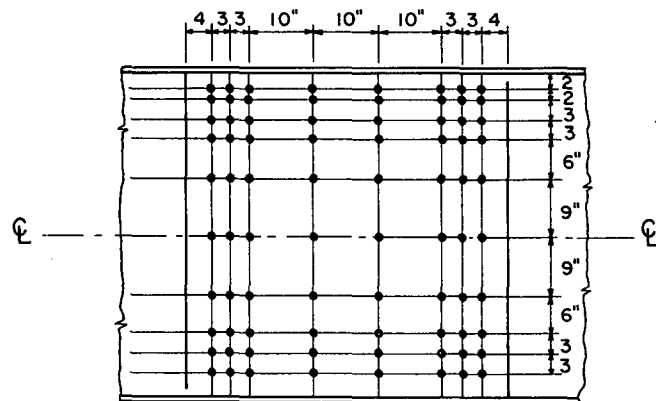
Fig. 3 Overall View of Test Setup



(a) SR4-A1 GAGES, GIRDERS F3 & F4



(b) SR4-A1 GAGES, GIRDER F5



(c) LOCATIONS OF LATERAL WEB DEFLECTION MEASUREMENTS (Typ.)

Fig. 4 Instrumentation

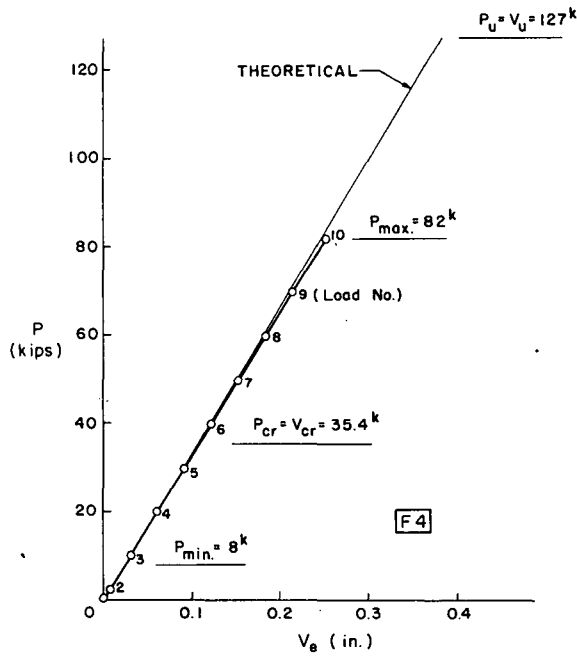
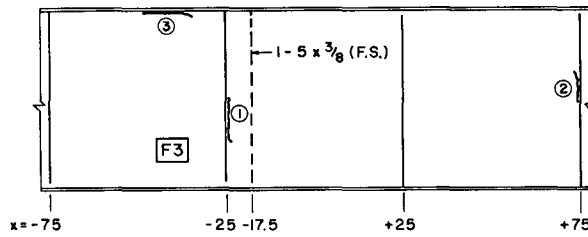
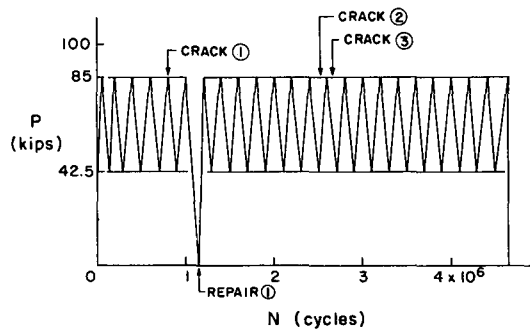


Fig. 5 Load-Deflection Curve, Girder F4

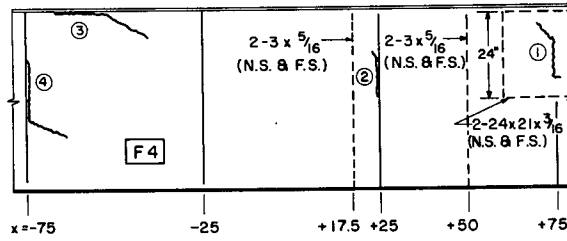


(a) Crack Location and Repair

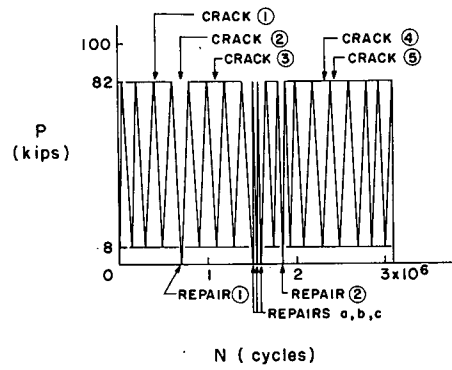


(b) Fatigue Test Sequence

Fig. 6 Testing of Girder F3

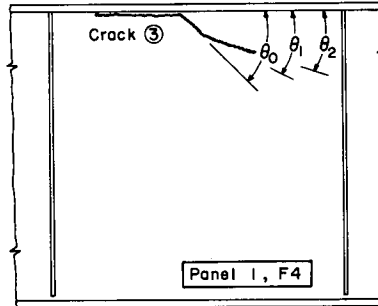


(a) Crack Location and Repair



(b) Fatigue Test Sequence

Fig. 7 Testing of Girder F4



(a)

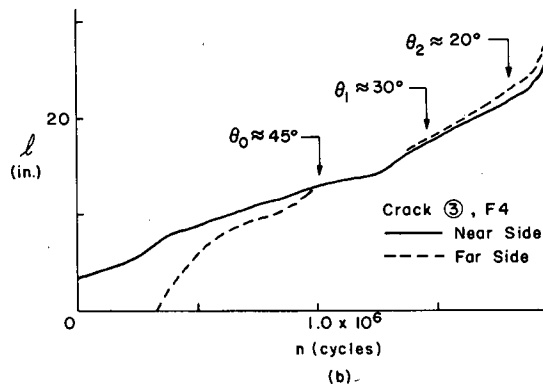
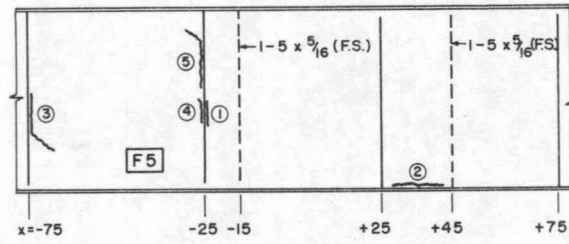
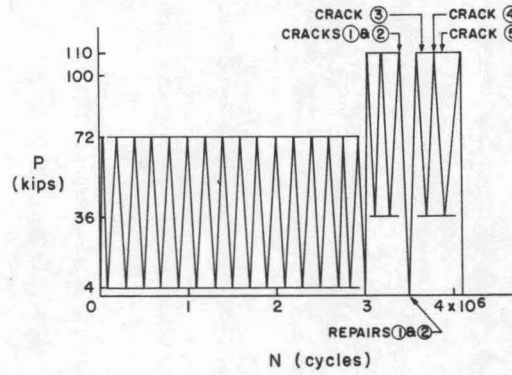


Fig. 8 Growth of Crack 3, Girder F4



(a) Crack Location and Repair



(b) Fatigue Test Sequence

Fig. 9 Testing of Girder F5

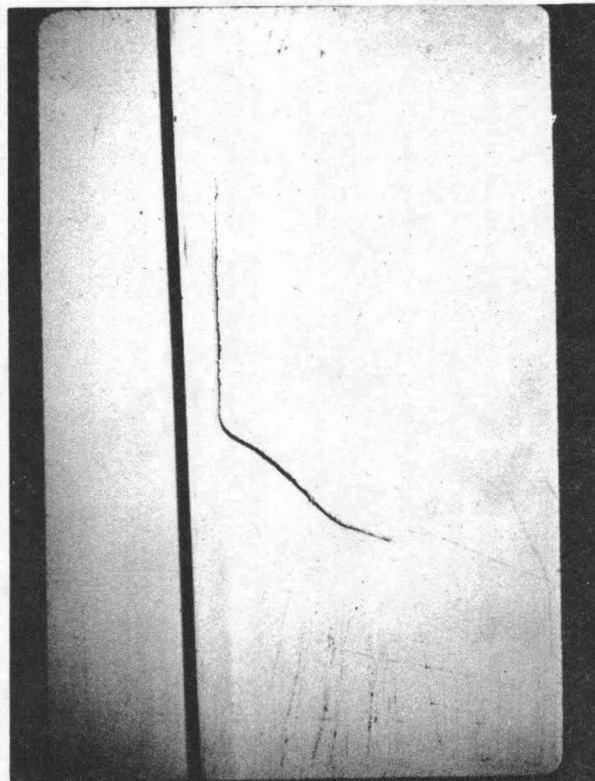


Fig. 10 Final Appearance, Crack 3, Girder F5

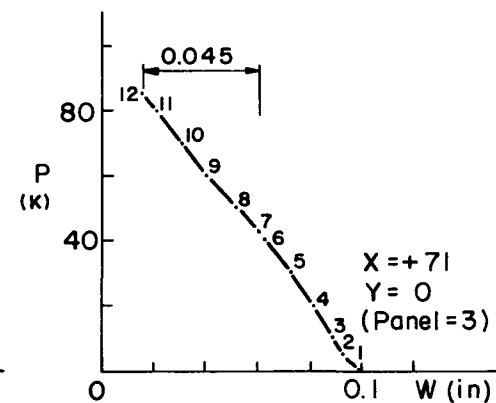
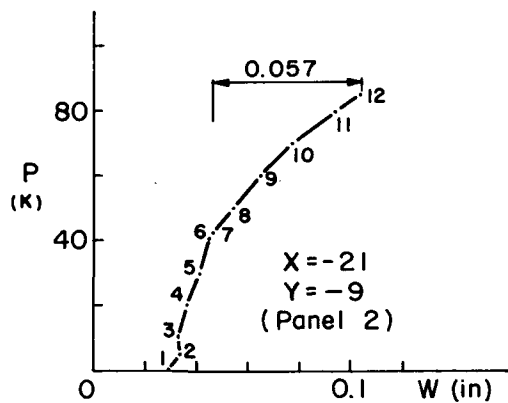
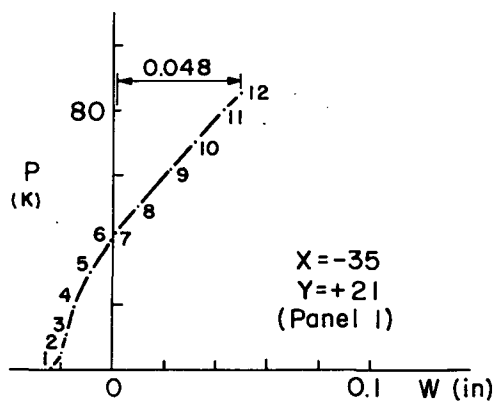
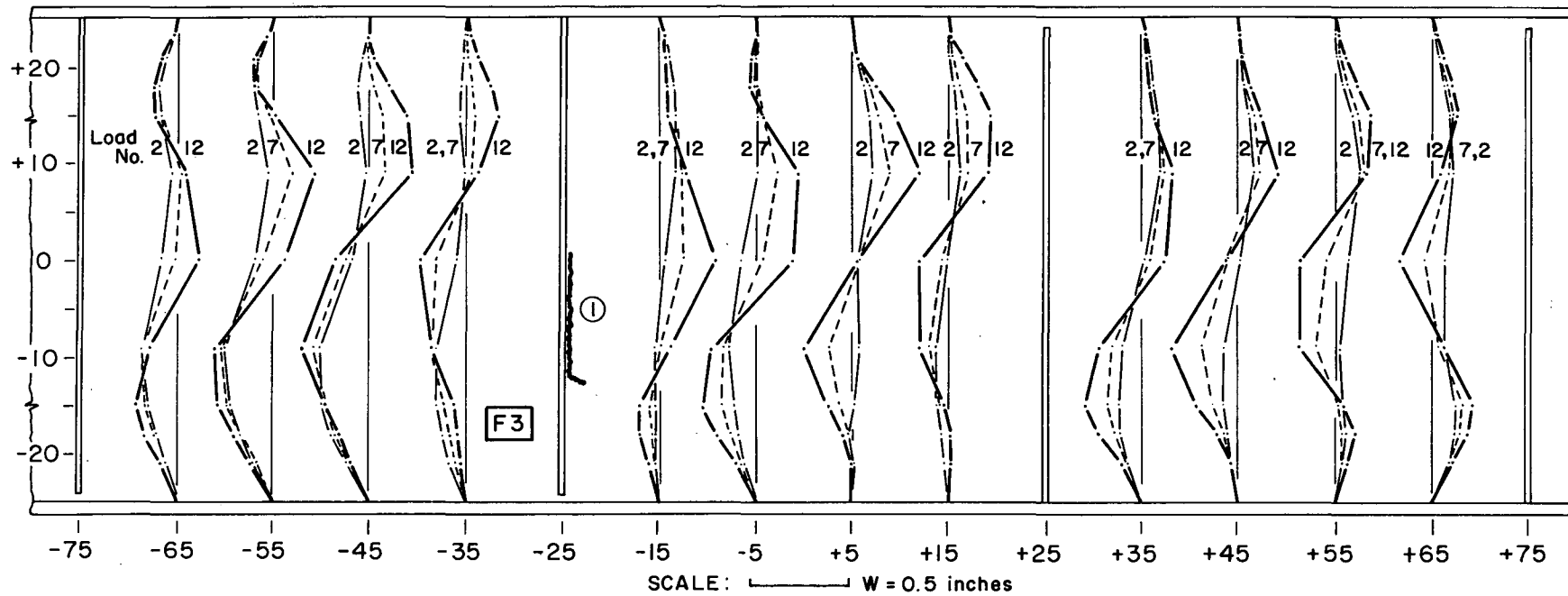


Fig. 11 Lateral Web Deflections, Girder F3

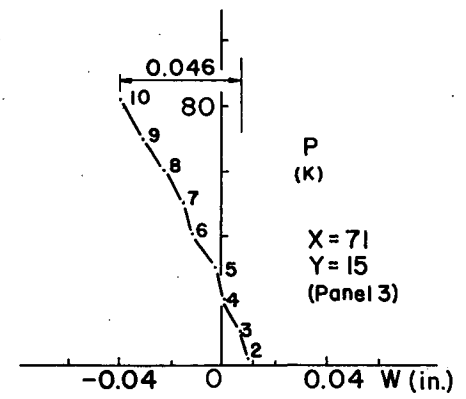
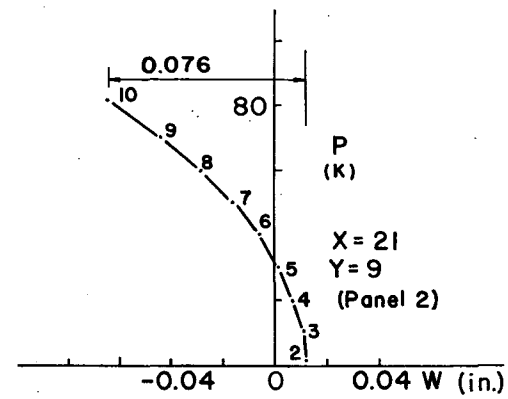
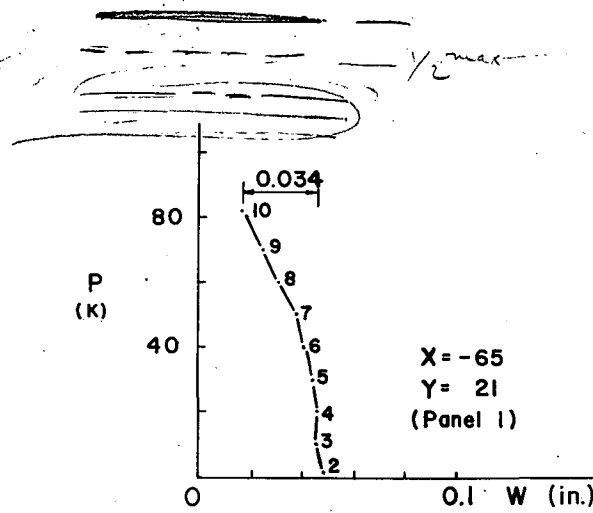
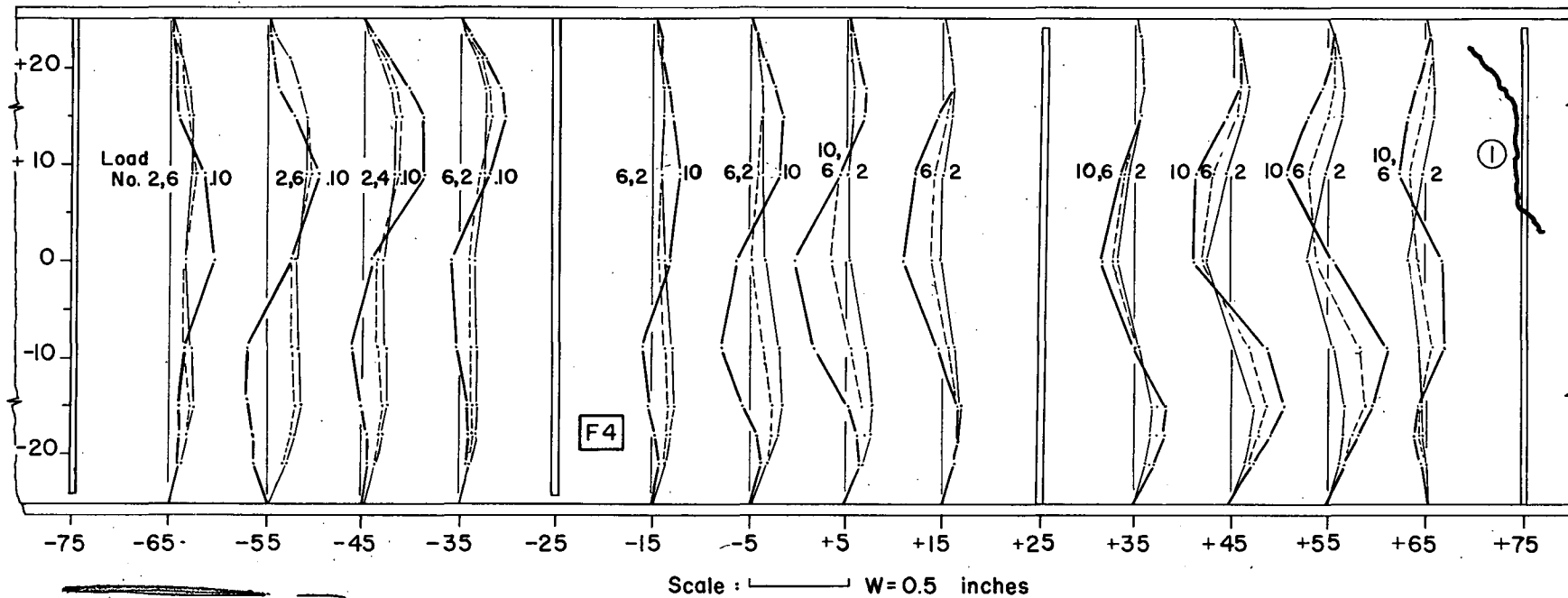


Fig. 12 Lateral Web Deflections, Girder F4

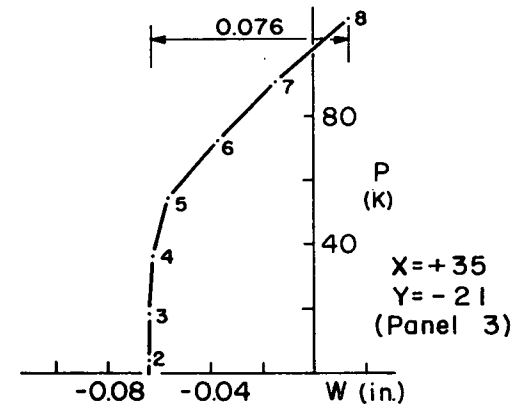
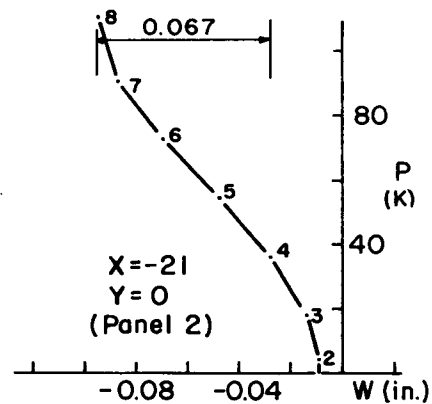
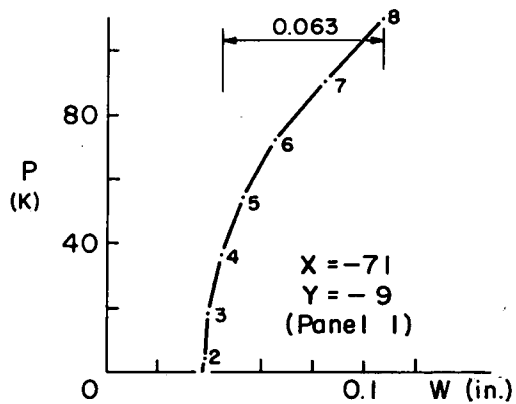
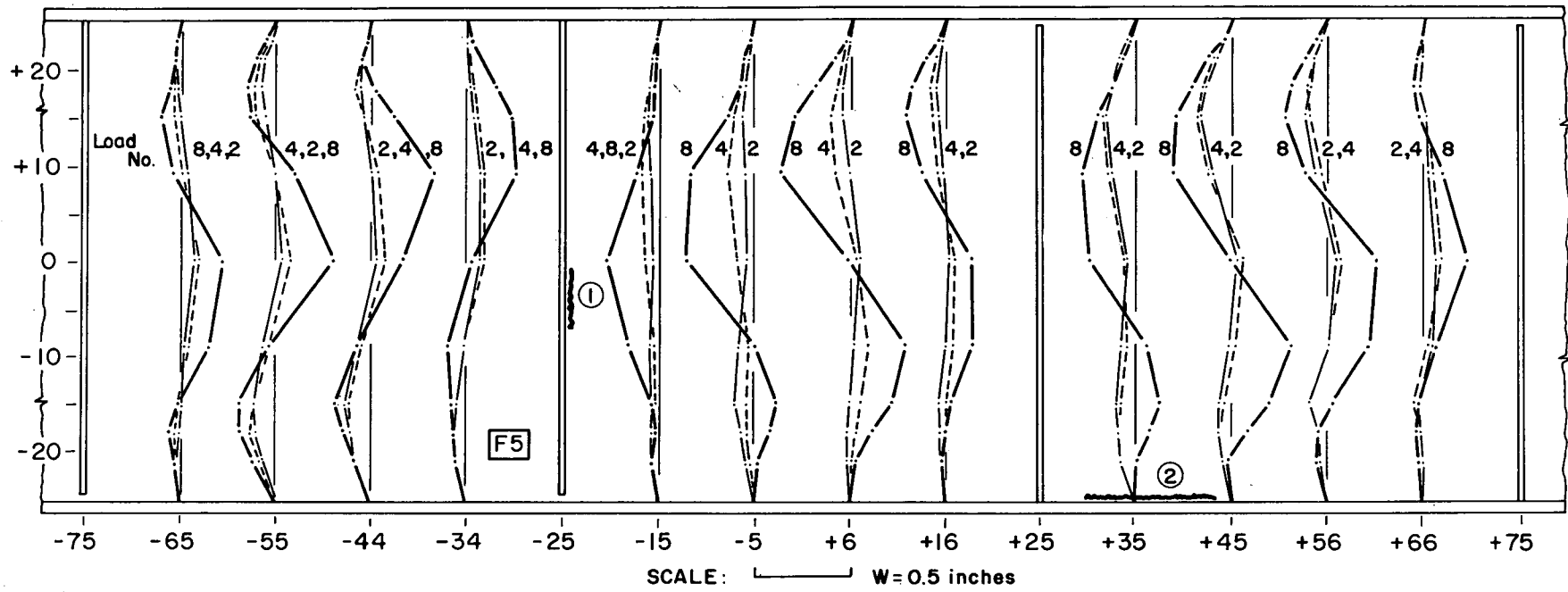
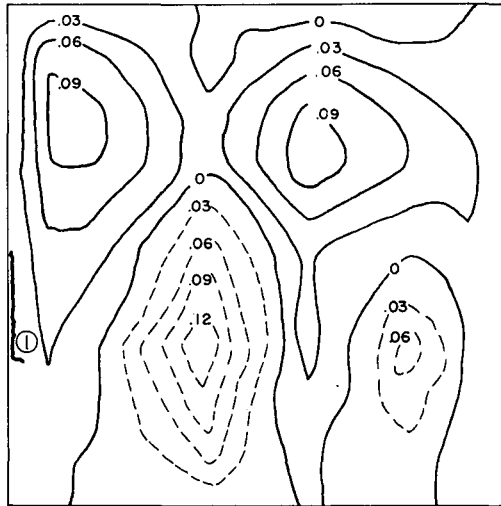
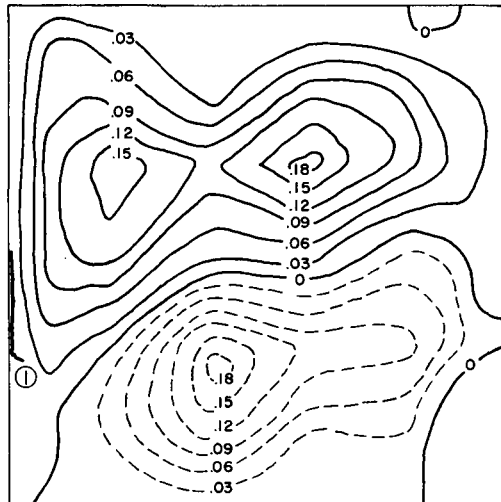


Fig. 13 Lateral Web Deflections, Girder F5

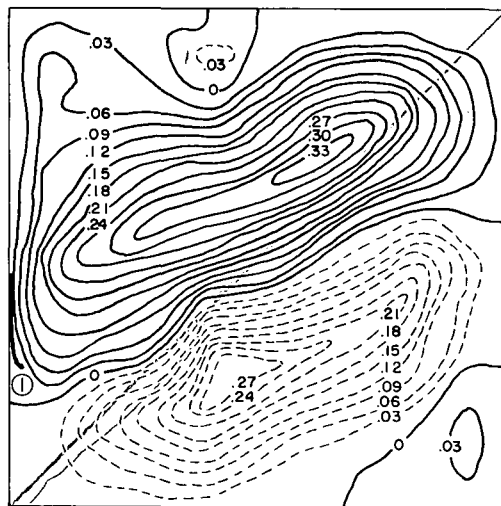


P = 5 kips
LOAD NO. 2

GIRDER F3
PANEL 2

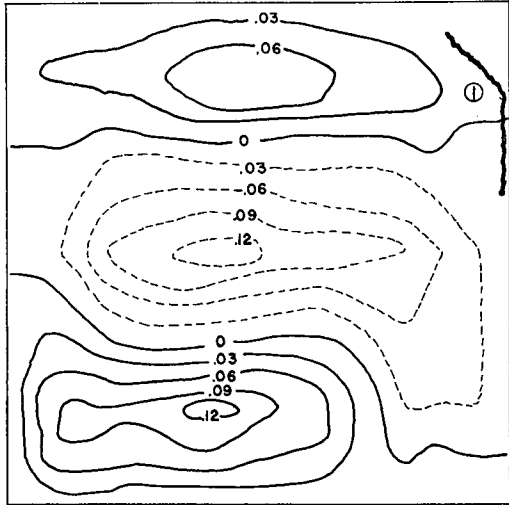


P = P_{min} = 42.5 kips
LOAD NO. 7



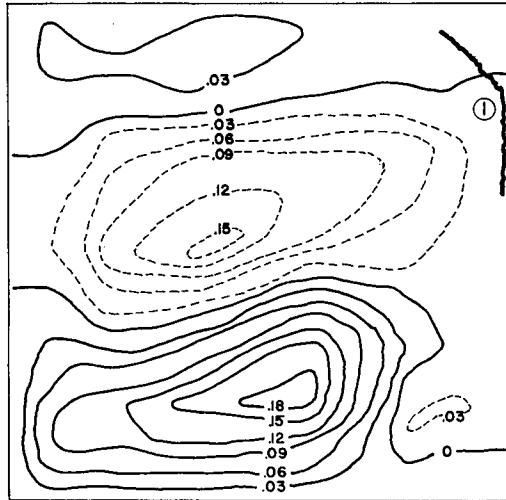
P = P_{max} = 85 kips
LOAD NO. 12

Fig. 14 Web Deflection Contours, Girder F3

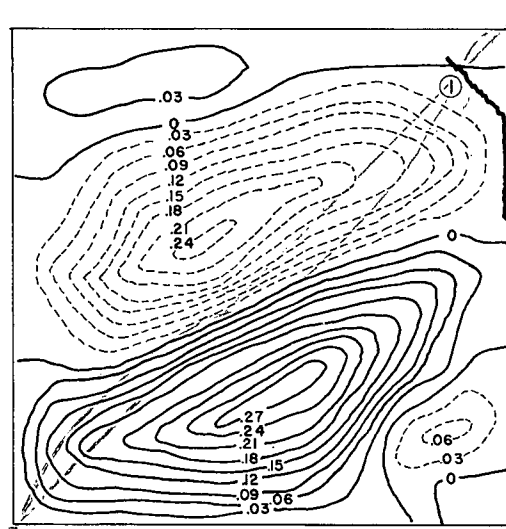


P = 2 kips
LOAD NO. 2

GIRDER F4
PANEL 3

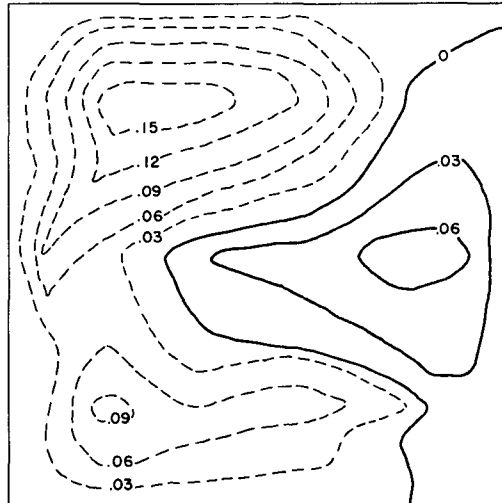


P = 40 kips
LOAD NO. 6



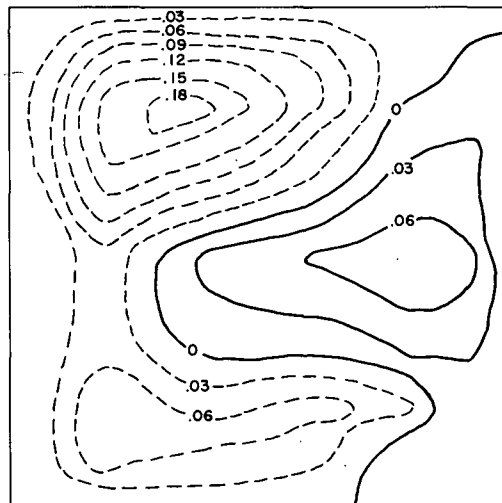
P = P_{MAX.} = 82 kips
LOAD NO. 10

Fig. 15 Web Deflection Contours, Girder F4

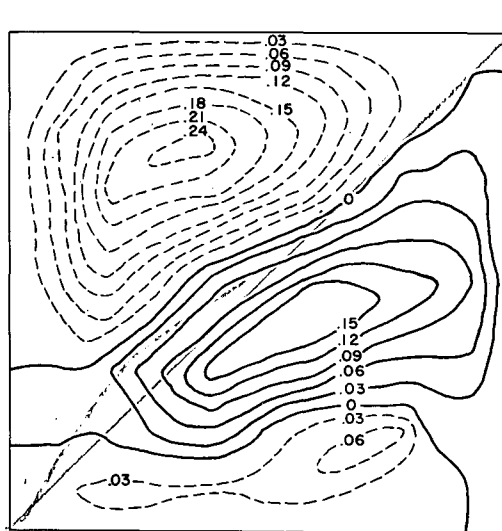


P = 4 kips
LOAD NO. 2

GIRDER F5
PANEL 3

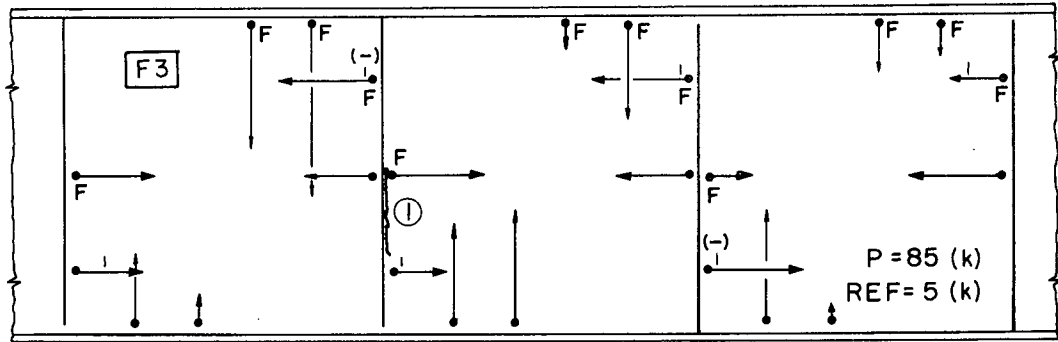


P = 36 kips
LOAD NO. 4

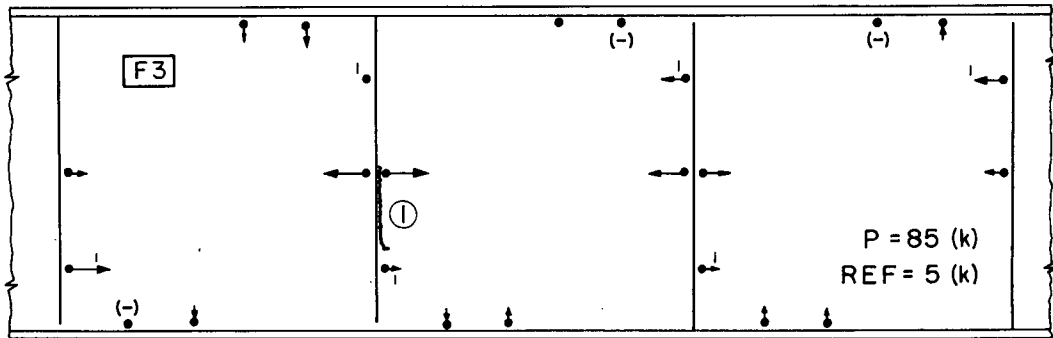


P = P_{max} = 72 kips
LOAD NO. 6

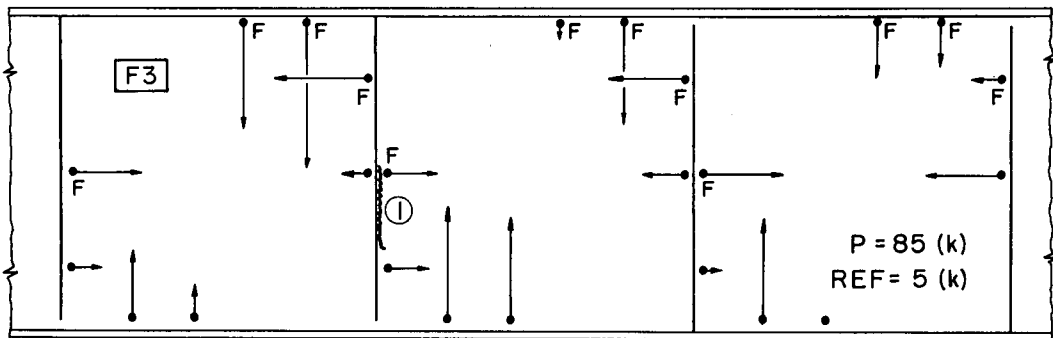
Fig. 16 Web Deflection Contours, Girder F5



a. Surface Stress



b. Membrane Stress

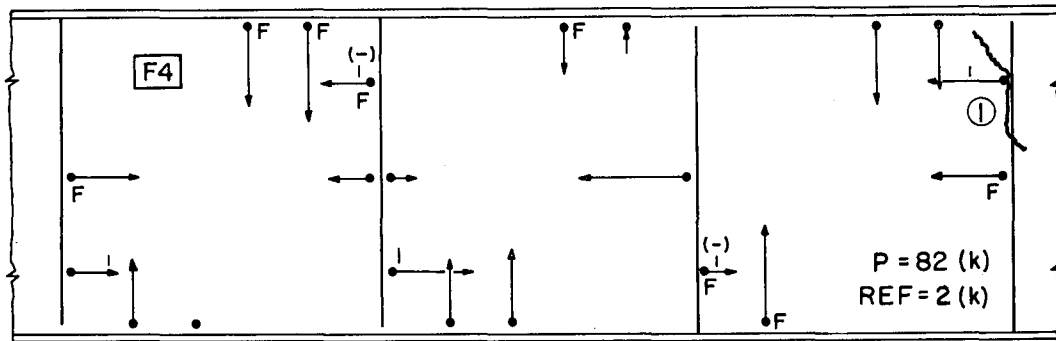


c. Secondary Bending Stress

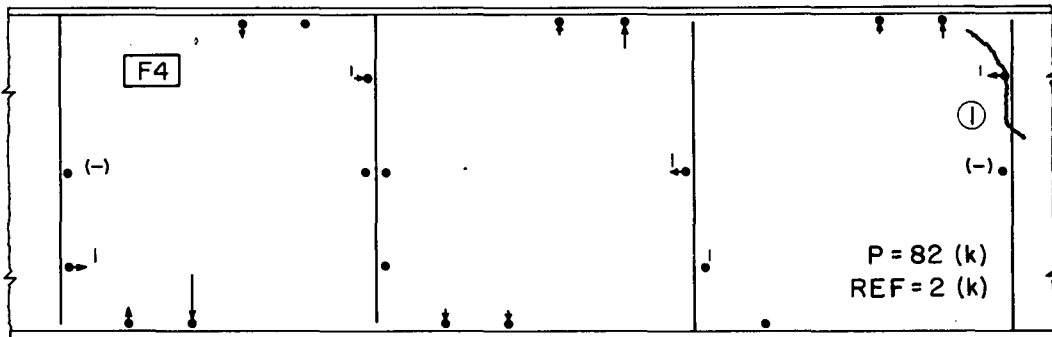
Scale: 0 20 (ksi)

Legend: Tension
 Compression

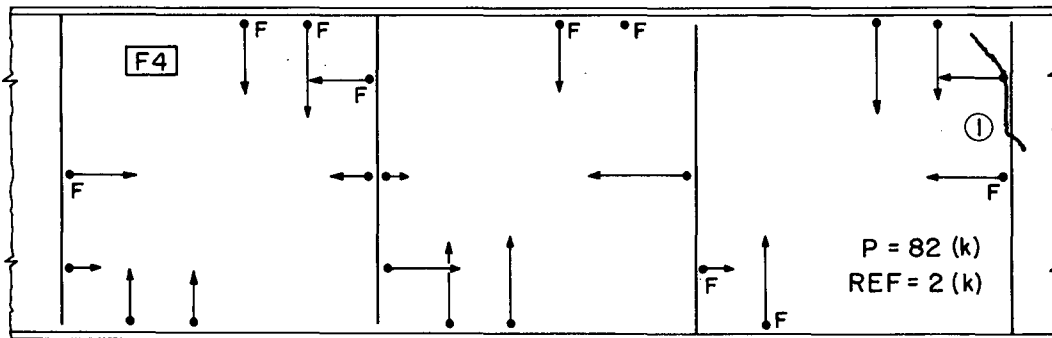
Fig. 17 Web Stresses Normal to Boundary, Girder F3



a. Surface Stress



b. Membrane Stress



c. Secondary Bending Stress

Scale: 0 ——— 20 (ksi)



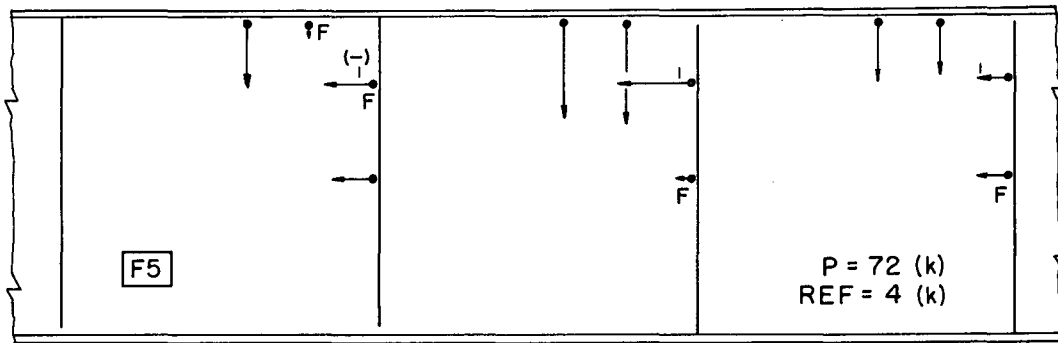
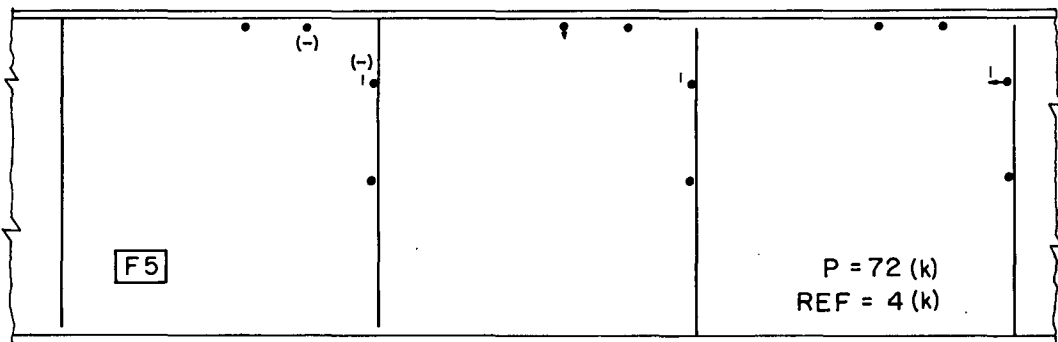
Legend:  Tension
 Compression

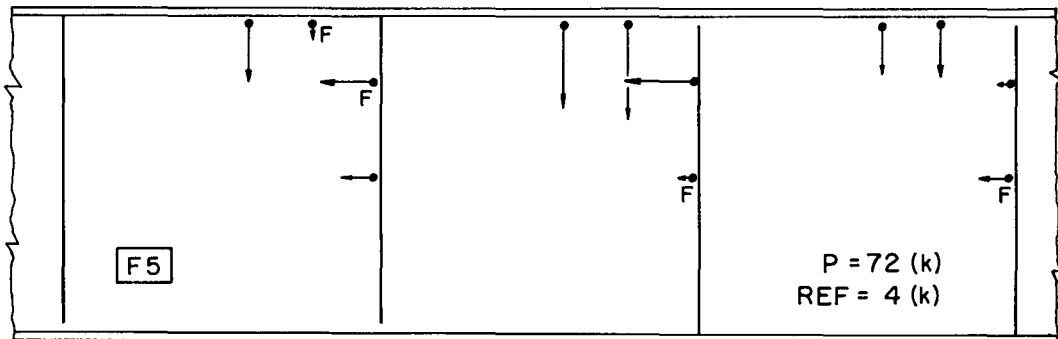
Fig. 18 Web Stresses Normal to Boundary, Girder F4



a. Surface Stress



b. Membrane Stress

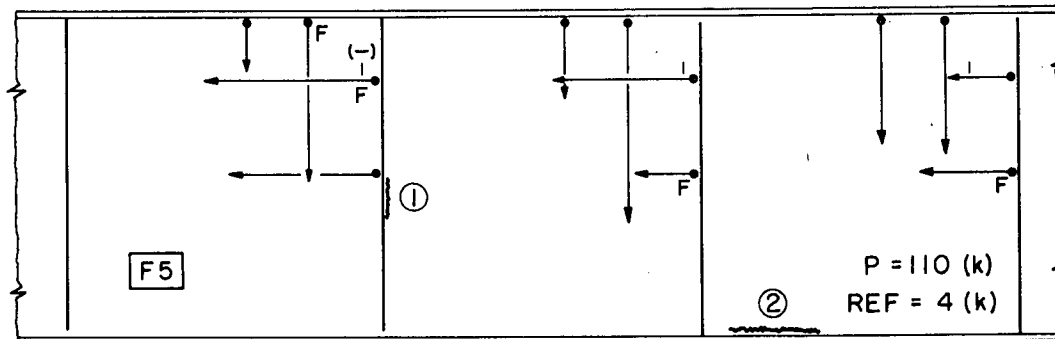


c. Secondary Bending Stress

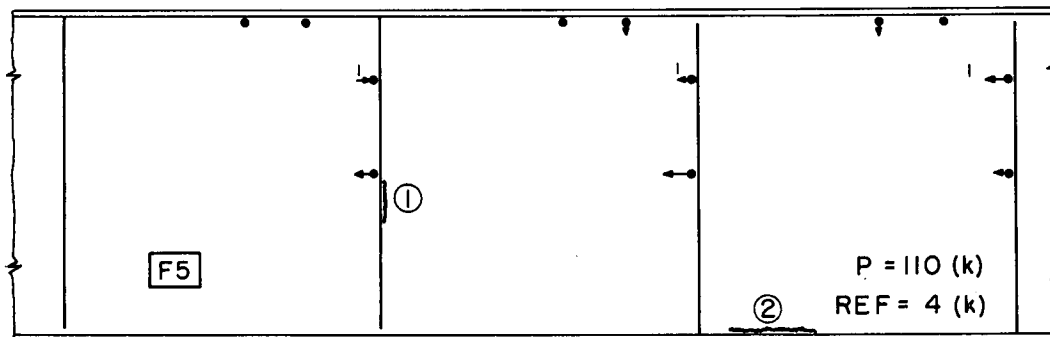
Scale: 0 ——— 20 (ksi)

Legend: ●——→ Tension
 ●——← Compression

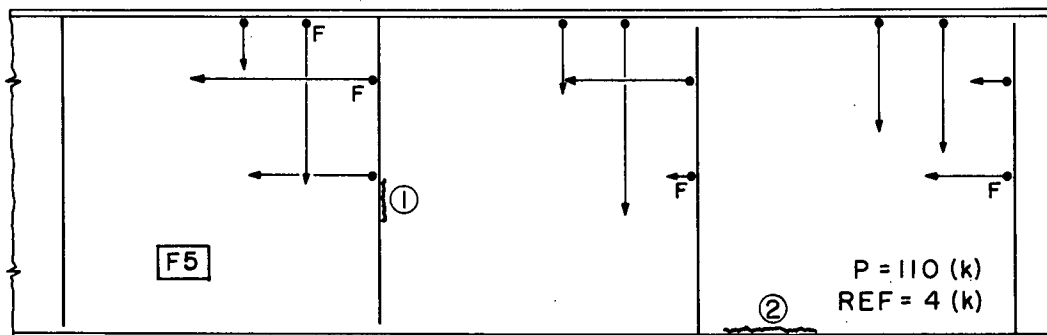
Fig. 19 Web Stresses Normal to Boundary, Girder F5



a. Surface Stress



b. Membrane Stress



c. Secondary Bending Stress

Scale: 0 ——— 20 (ksi)

Legend: Tension
 Compression

Fig. 20 Web Stresses Normal to Boundary, Girder F5

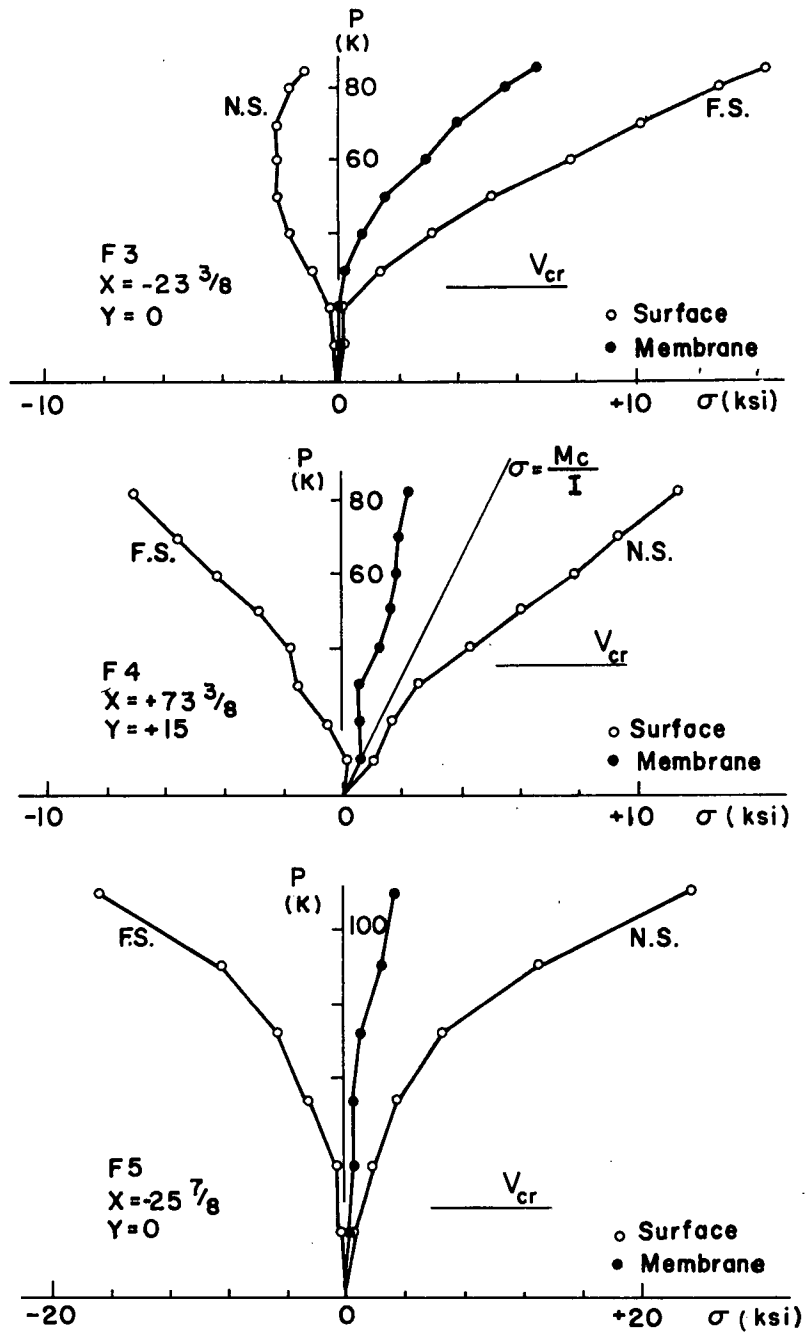
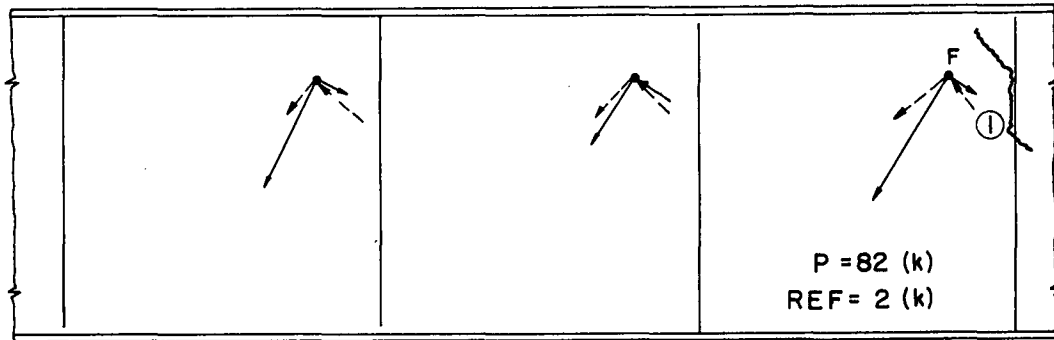
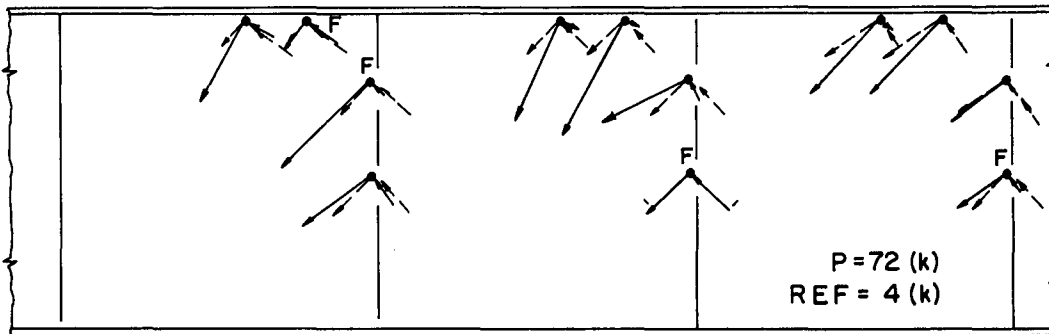


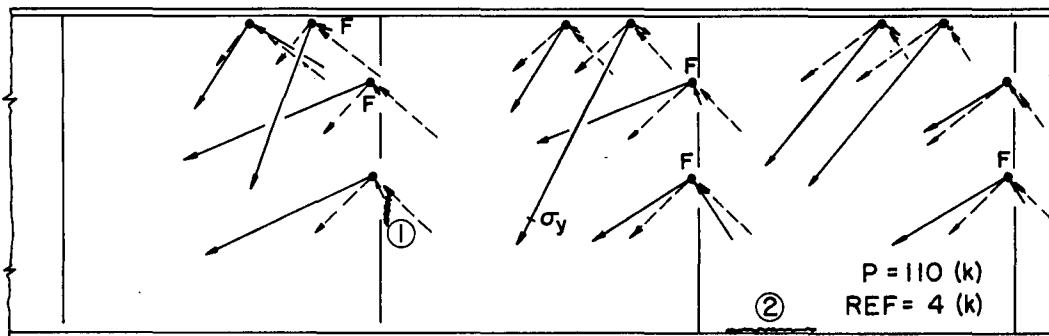
Fig. 21 Web Stresses Versus Applied Load



a. Girder F4



b. Girder F5

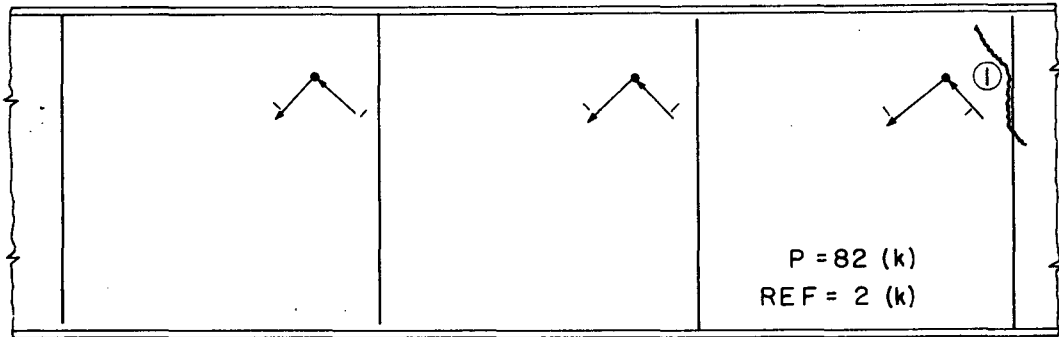


c. Girder F5

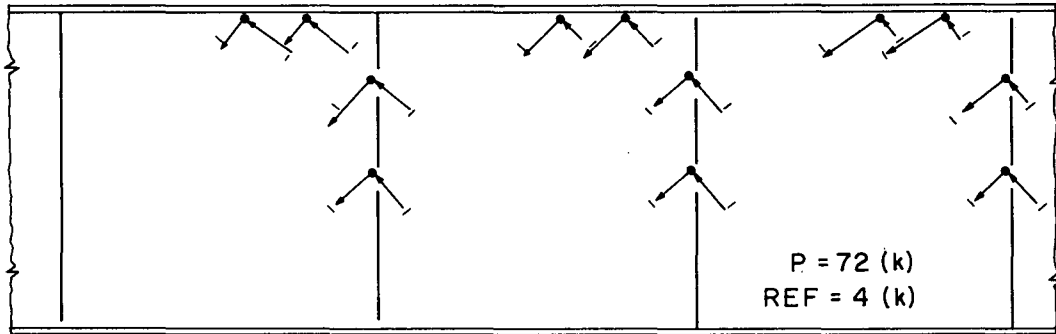
Scale: 0 20 (ksi)

- Tensile
- Compressive
- - Bm. Theory Predict.

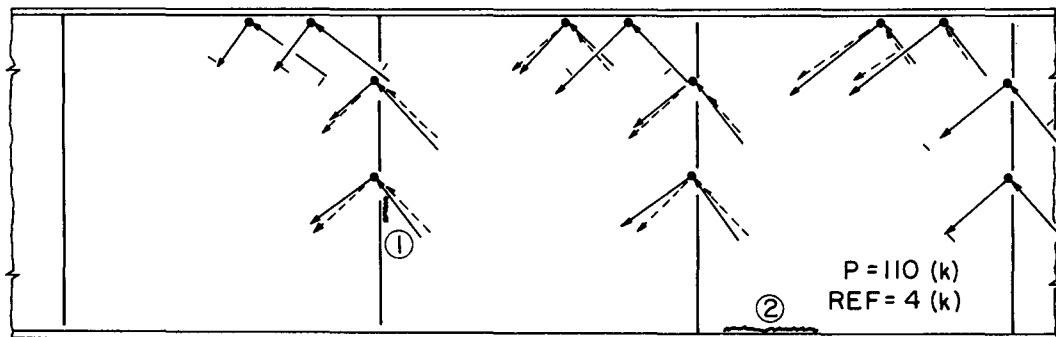
Fig. 22 Principal Surface Stresses of the Web



a. Girder F4



b. Girder F5



c. Girder F5

Scale: 0 ——— 20 (ksi)

Legend:
 ●——> Tensile
 ●——< Compressive
 ●---> Bm. Theory Predict

Fig. 23 Principal Membrane Stresses in the Web

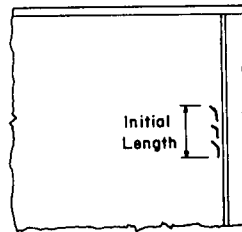
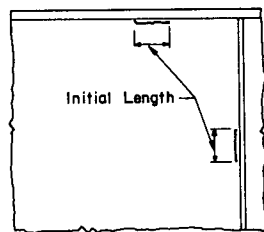
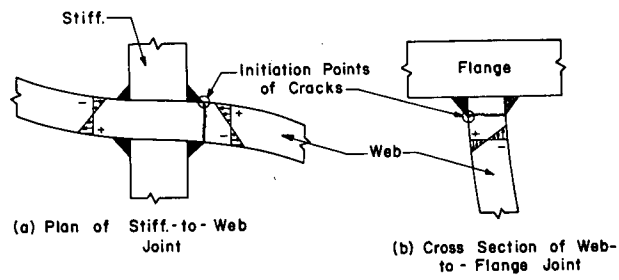


Fig. 24 Location and Appearance of Cracks When First Observed

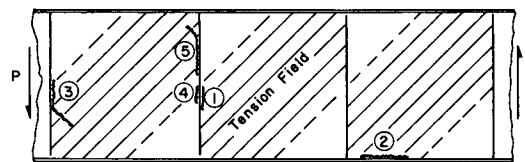
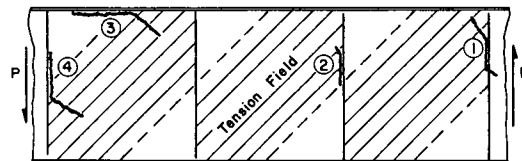
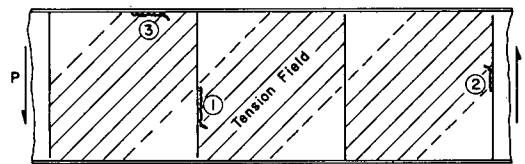


Fig. 25 Cracks and the Idealized Tension Field

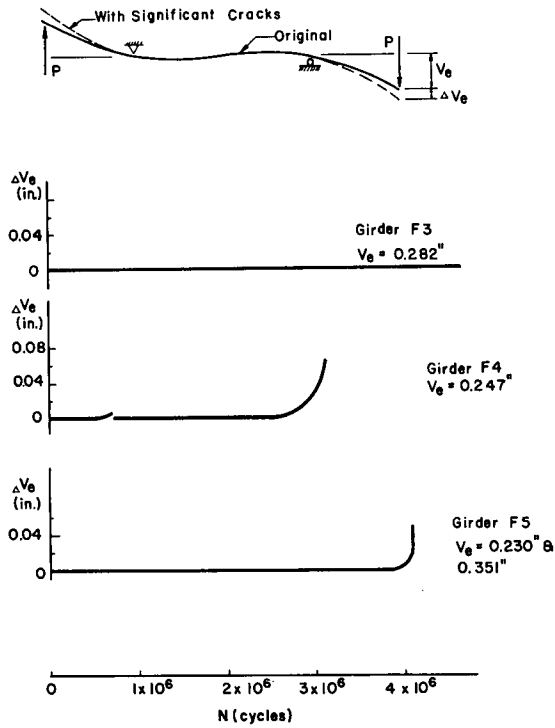


Fig. 26 Girder Stiffness Versus Applied Load Cycles

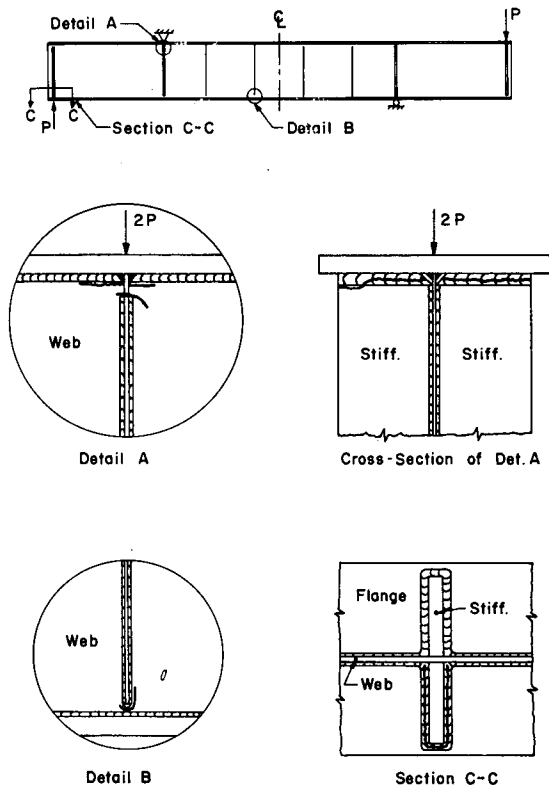


Fig. 27 "Minor" Cracks of Girder F4

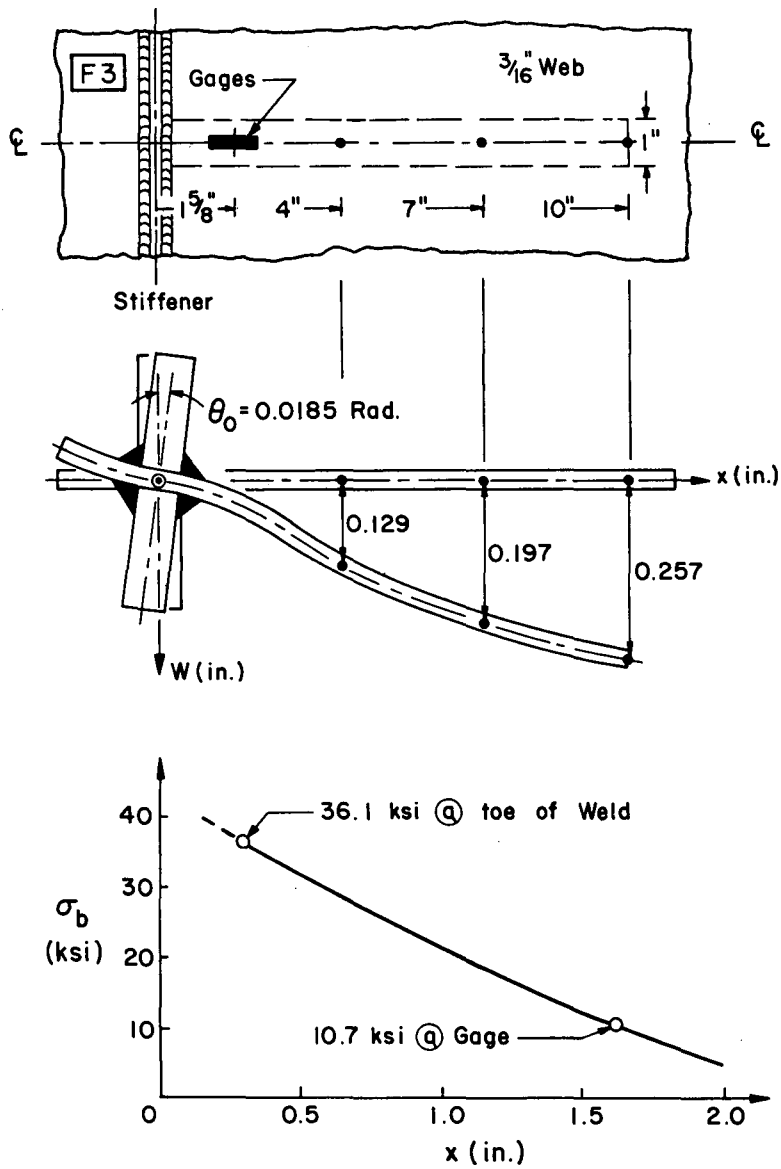


Fig. 28 Secondary Bending Stress Approximation

REFERENCES

1. K. Basler and B. Thürlimann
STRENGTH OF PLATE GIRDERS IN BENDING
Proceedings, ASCE, Vol. 87, No. ST6, 1961
2. K. Basler
STRENGTH OF PLATE IN SHEAR
Proceedings, ASCE, Vol. 87, No. ST7, 1961
3. K. Basler
STRENGTH OF PLATE GIRDERS UNDER COMBINED BENDING AND SHEAR
Proceedings, ASCE, Vol. 87, No. ST7, 1961
4. K. Basler, B. T. Yen, J. A. Mueller and B. Thürlimann
WEB BUCKLING TESTS ON WELDED PLATE GIRDERS
Bulletin No. 64, Welding Research Council, New York
September 1960
5. P. B. Cooper, H. S. Lew and B. T. Yen
TESTS ON WELDED HIGH STRENGTH STEEL PLATE GIRDERS SUBJECTED
TO SHEAR
Lehigh University, Fritz Engineering Laboratory Report
No. 251.29, December 1961
6. B. T. Yen and P. B. Cooper
FATIGUE TESTS OF WELDED PLATE GIRDERS
AWS Welding Journal, Vol. 42, No. 6, June 1963
7. B. T. Yen
ON THE FATIGUE STRENGTH OF WELDED PLATE GIRDERS
Lehigh University, Fritz Engineering Laboratory
Report No. 303.1, November 1963
8. H. S. Reemsnyder
THE FATIGUE BEHAVIOR OF STRUCTURAL STEEL WELDMENTS.
A LITERATURE SURVEY
Lehigh University, Fritz Engineering Laboratory Report
No. 284.1, November 1961